

Secondary Precious Metal Enrichment by Steam-Heated Fluids in the Crofoot-Lewis Hot Spring Gold-Silver Deposit and Relation to Paleoclimate

SHANE W. EBERT^{†,*}

Key Centre for Strategic Mineral Deposits, Department of Geology and Geophysics, University of Western Australia, Nedlands, Western Australia 6907, Australia

AND ROBERT O. RYE

U.S. Geological Survey, P.O. Box 25046, Mail Stop 963, Denver Federal Center, Denver, Colorado 80225

Abstract

The Crofoot-Lewis deposit is an adularia-sericite-type (low-sulfidation) epithermal Au-Ag deposit, whose well-preserved paleosurface includes abundant opaline sinters, widespread and intense silicification, bedded hydrothermal eruption breccias, and a large zone of acid sulfate alteration. Radiogenic isotope ages indicate that the system was relatively long-lived, with hydrothermal activity starting around 4 Ma and extending, at least intermittently, for the next 3 m.y.

Field evidence indicates that the surficial zone of acid sulfate alteration formed in a steam-heated environment within an active geothermal system. A drop in the water table enabled descending acid sulfate waters to leach Au and Ag from zones of low-grade disseminated mineralization, resulting in the redistribution and concentration of Au and Ag into ore-grade concentrations. These zones of secondary Au-Ag enrichment are associated with opal + alunite + kaolinite + montmorillonite ± hematite and were deposited in open space fractures at, and within a few tens of meters below, the paleowater table.

The stable isotope systematics of alunite and kaolinite in the steam-heated environment are relatively complex, due to variations in the residence time of aqueous SO₄ that formed from the oxidation of H₂S prior to precipitation of alunite, and the susceptibility of fine-grained kaolinites to hydrogen isotope exchange with later waters. Most of the alunites are enriched in ³⁴S relative to early sulfide minerals, reflecting partial S isotope exchange between aqueous SO₄ and H₂S. About half of the alunites give reasonable calculated $\Delta^{18}\text{O}_{\text{SO}_4\text{-OH}}$ temperatures for a steam-heated environment indicating O isotope equilibrium between aqueous SO₄ and water. The $\delta\text{D}_{\text{H}_2\text{O}}$ values of the hydrothermal fluids varied by almost 60 per mil over the life of the meteoric water-dominated system, suggesting significant climate changes.

Mineralization is believed to have resulted from large-scale convection of meteoric water controlled largely by basin and range fractures and a high geothermal gradient with H₂S for Au complexing derived from organic matter in basin sediments. A wet climate resulted in the formation of a large inland lake which provided abundant recharge water for the hydrothermal system. A fluctuating water table controlled by changing climatic conditions enabled steam-heated acid sulfate fluids to overprint lower grade mineralization resulting in ore-grade precious metal enrichment.

Introduction

THE Crofoot-Lewis mine is an adularia-sericite (Heald et al., 1987) or low-sulfidation (Hedenquist, 1987) type epithermal Au-Ag deposit, located in northwestern Nevada, near the abandoned town of Sulphur (Fig. 1). Radiometric ages show that the hydrothermal system was young (4.0–0.7 Ma) and consequently many features of the paleosurface remain, including sinter, bedded hydrothermal eruption breccias, and surficial acid sulfate alteration. Current Au-Ag (Hg) mining by Hycroft Resources and Development Incorporated commenced in 1987, with proven and probable reserves, as of October 1994, of 57.8 million tons (Mt) grading 0.65 g/t Au and containing 31,185 kg Au. Mining is by open pit and cyanide heap-leach methods. Current annual production is approximately 2,835 kg (100,000 oz) Au, 8,500 kg (300,000 oz) Ag, and 13,600 kg Hg.

It has long been recognized that paleoclimate has played

a major role in the genesis of various metal, industrial mineral, and strategic fuel deposits (Cronin et al., 1983), but only recently has a link been suggested between paleoclimate and epithermal systems (Berger and Henley, 1989). The Great Basin of the western United States is susceptible to the accumulation of large volumes of surface water during periods of abundant precipitation, and large inland lakes have periodically formed within the Great Basin at least as far back as late Tertiary times (Forester, 1991). These inland lakes expanded and contracted according to paleoclimatic conditions (Smith, 1984; Forester, 1991), reflecting major changes in the regional water table. Changes in the level of the water table can have a major effect on the surficial environment of active epithermal systems, resulting in the overprinting of different alteration assemblages (Simmons, 1991).

In this paper we describe in detail the acid sulfate alteration and use field relations, combined with light stable isotope data, K-Ar dating, paleoclimate records, and geologic constraints, to propose that fluctuations in the water table during the formation of the Crofoot-Lewis deposit enabled acid sulfate alteration to overprint weakly mineralized near-surface silicification, resulting in the leaching, redistribution, and sec-

[†] Corresponding author: email, sebert@compuserve.com

* Present address: Hot Spring Gold Corporation, 4650 Sierra Madre #813, Reno, Nevada 89502.

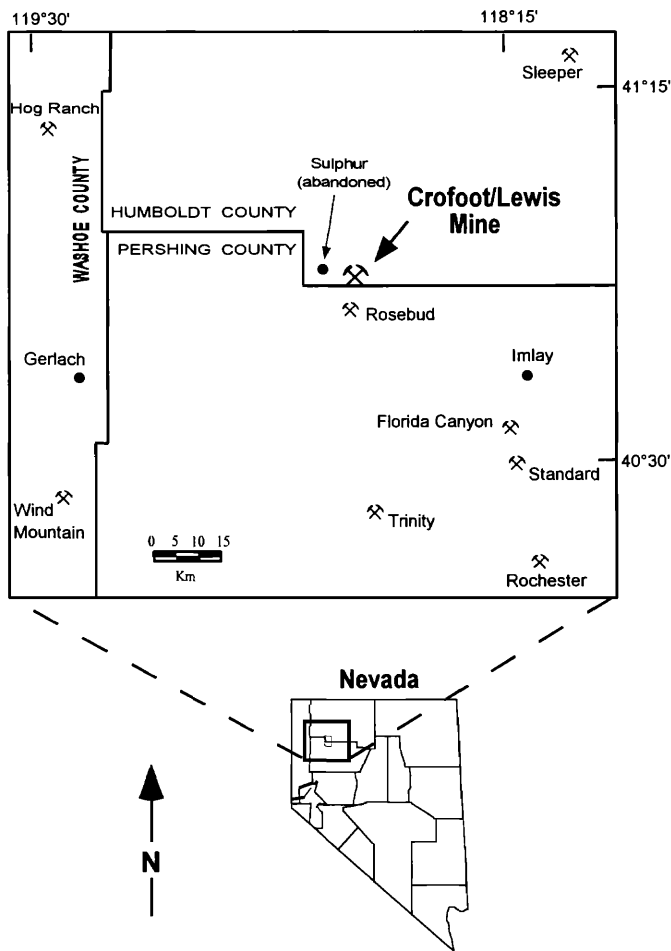


FIG. 1. Location map of the Crofoot-Lewis mine, Humboldt County, Nevada, showing adjacent precious metal deposits.

ondary enrichment of Au and Ag. In addition we propose a genetic model for the formation of young hot spring gold deposits in the Great Basin, which has important implications for exploration, and to our knowledge, has not been previously proposed.

Geology

A more detailed description of the geology, mineralization, and secondary Au enrichment at the Crofoot-Lewis mine is given in Ebert et al. (1996), and only a brief summary is presented here.

Regional geology

The regional geology surrounding the Sulphur district is dominated by late Cenozoic basin-and-range extensional faulting. The major rock types in the region have been mapped and described by Willden (1964) and Johnson (1977) and are summarized in Figure 2. Triassic to Jurassic rocks of the Auld Lang Syne Group (Burke and Silberling, 1974) are widespread through the region. The Auld Lang Syne Group is a thick sequence of variably metamorphosed metasedimentary rocks, consisting of phyllite, slate, metasiltstone, fine-grained quartzite, and local hornfels and is part of the Jungo Mesozoic allochthonous terrane (e.g., Oldow, 1984).

Tertiary rocks are abundant in the surrounding ranges, and include volcanic, volcanoclastic, intrusive, and fresh-water sedimentary rocks (Willden, 1964). Igneous rocks are common and range in composition from olivine basalt to rhyolite. Sedimentary rocks are abundant in the downdropped basins that formed during the development of basin-and-range structure (Stewart, 1980). The sedimentary rocks within the Black Rock Desert basin adjacent to the ore deposit are not exposed. A general description of these rocks is based on drill cuttings from a 2,417-m-deep oil exploration well drilled in the basin 12 km north of the Crofoot-Lewis mine (Garside et al., 1988). The late Cenozoic (Miocene-Holocene) basin sediments and sedimentary rocks in the Black Rock Desert basin contain traces of oil and gas (Garside et al., 1988) and are interpreted to be 2,160 m thick. From 1,600 to 1,775 m, the rocks are predominantly poorly consolidated to unconsolidated siltstone. From 1,775 to 2,160 m, the cuttings are tuffs, clays, shale, sandstone, conglomerate, marl, and limestone, locally containing traces of pyrite. From 2,160 m to the bottom of the hole (2,417 m) volcanic rocks were encountered.

Unconsolidated sedimentary material of Pliocene and younger age (<6 Ma) forms widespread alluvial fan, stream terrace, flood plain, valley flat, and playa deposits that grade from coarse grained near the range fronts to fine silt and clay in the valleys. Large inland lakes occupied many of the present-day valleys of Nevada during the Pleistocene, and many of the presently exposed playa and shoreline deposits originated in these lakes (Morrison, 1964).

Deposit geology

A series of subparallel basin-and-range-type normal faults offset rock types and control much of the near-surface mineralization and alteration in the district (Figs. 3, 4). These faults strike approximately north (N 15°–30° E) and dip 55° to 85° to the west. Northwest- and west-striking transfer or relay faults locally cause minor offsets in ore zones and along north-striking faults.

The oldest rock unit in the Sulphur district is the Mesozoic Auld Lang Syne Group, which is present below the deposit (Fig. 4) and crops out 5 km east of the mine site. Here the unit consists of laminated slate and siltstone. In places, the unit is highly contorted and folded, and graphite is abundant along bedding-foliation planes.

Unconformably overlying the Auld Lang Syne Group is the Tertiary Kamma Mountains group (informally named by Wallace, 1987). This group consists of predominantly east-dipping felsic volcanic, volcanoclastic, and pyroclastic rocks. Rhyolite lava flows (locally domes), with well-developed flow banding, are common in the sequence. Minor dacitic to andesitic rocks, and rhyolitic flow breccias and tuffaceous units occur locally.

The Kamma Mountains group is overlain by the Sulphur group (informally named by Wallace, 1987), which consists of Pliocene to Pleistocene sediments and sedimentary rocks. The Sulphur group is divided into the Lower Sulphur group, the Camel conglomerate, the Crofoot breccia, and sinter deposits. The Lower Sulphur group consists of fine-grained siltstones, tuffs, sandstones, and minor pebble conglomerates. The Camel conglomerate is a poorly sorted matrix-supported conglomerate with clasts up to 25 cm in size, averaging 1.5

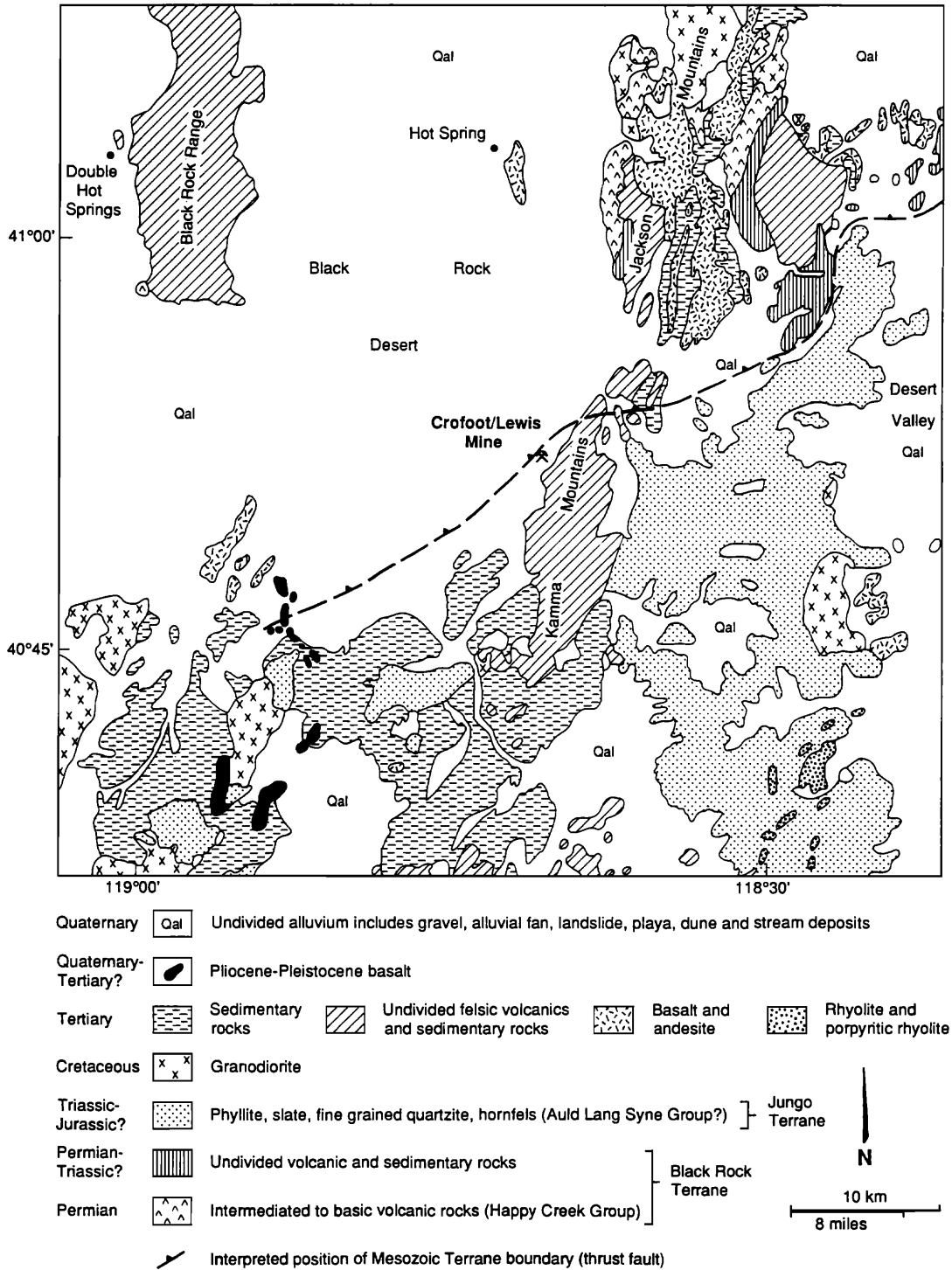


FIG. 2. Generalized regional geology of south-central Humboldt and north-central Pershing Counties. Geology from Willden (1964) and Johnson (1977).

cm. The clasts in this unit are derived from the Auld Lang Syne Group or the Kamma Mountains group, and lithification is a product of hydrothermal alteration. Crofoot breccia refers to hydrothermal eruption deposits that are pervasively altered and abundant near the surface at the Crofoot-Lewis deposit. The sinter deposits consist of beds of massive opaline and

chalcedonic silica interbedded with silicified Camel conglomerate. Sinter beds range from 30 cm to several meters in thickness and occur interbedded with Crofoot breccia and Camel conglomerate, having a maximum cumulative thickness of about 45 m. Individual sinter beds are flat lying and extend for hundreds of meters. The sinters typically contain

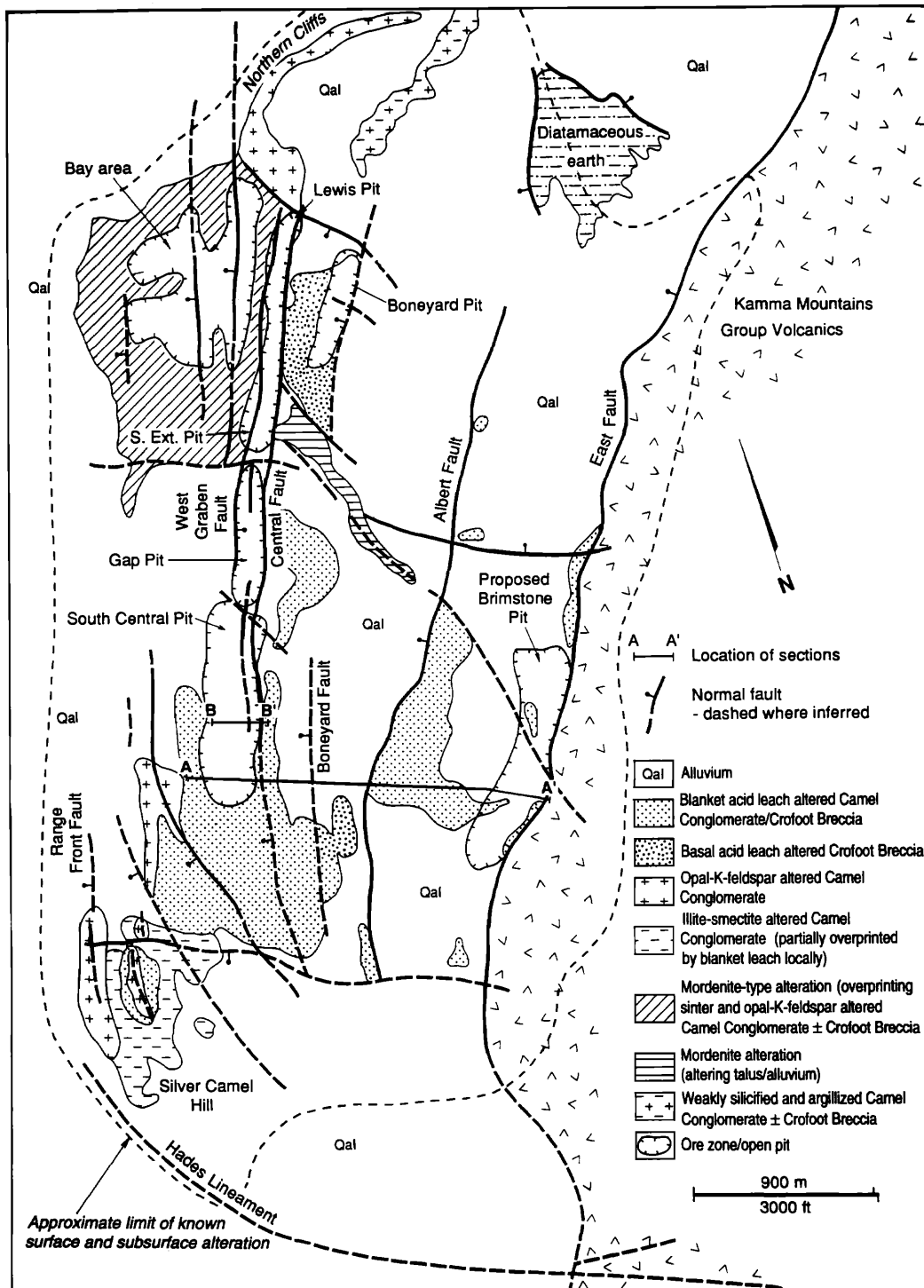


FIG. 3. Simplified map of the Sulphur district showing structure, hydrothermal alteration, ore zones, and limit of hydrothermal alteration.

abundant opalized aquatic reed casts that are often in an upright or growth position. The presence of opalized aquatic plant material and the flat-lying and extensive nature of these deposits indicate that they are shallow-water lacustrine deposits, probably analogous to the subaqueous "pool sinter" described at Buckskin Mountain, Nevada (Vikre, 1985).

Hydrothermal Alteration

Introduction

Figures 3 and 4 summarize the distribution of hydrothermal alteration in the Sulphur district. Hydrothermally altered rocks are extensive in the district, covering an area greater

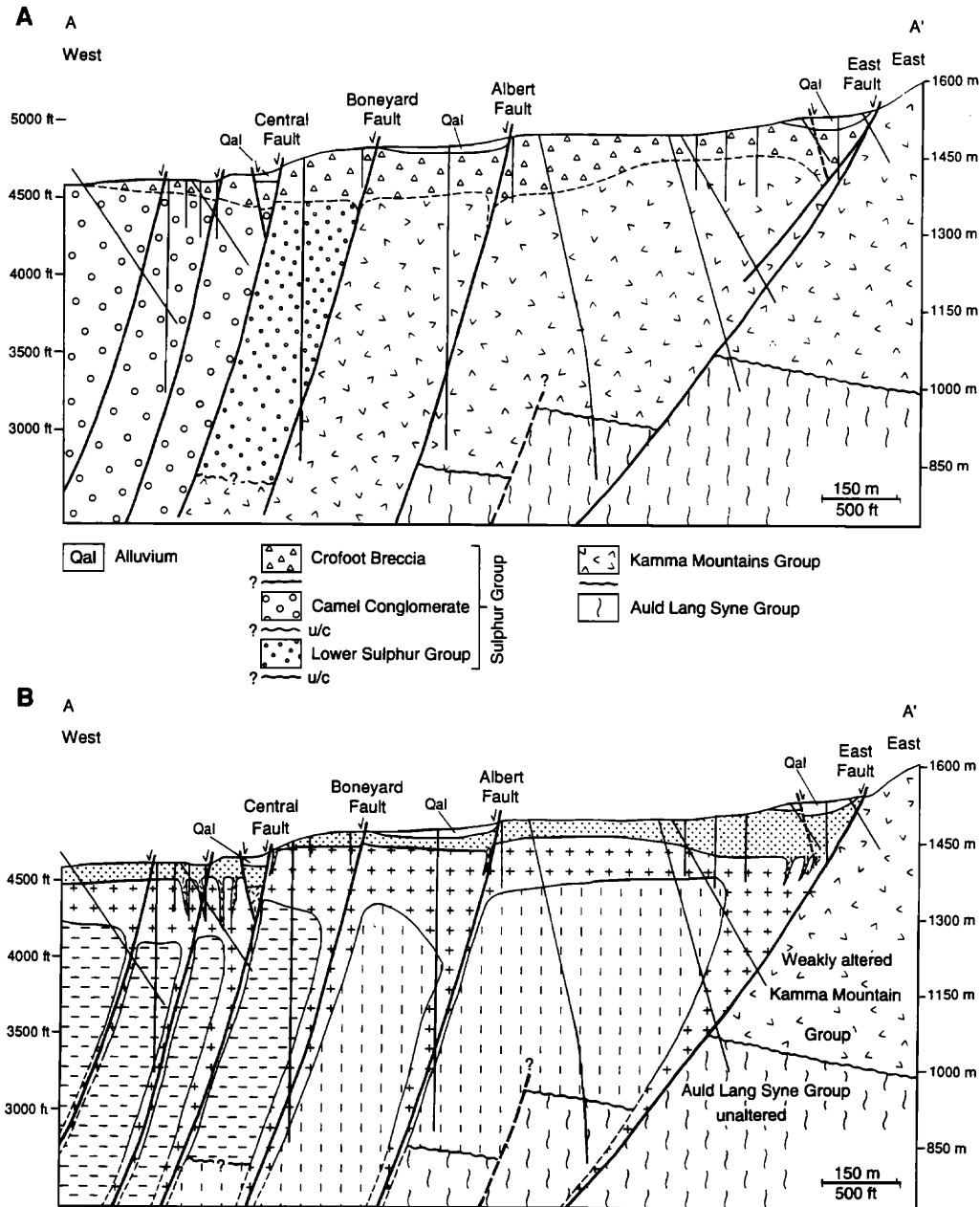


FIG. 4. Cross section through the Crofoot-Lewis deposit showing (A) rock types and (B) hydrothermal alteration.

than 3 by 7 km at or near the surface and extending to depths greater than 600 m, the limit of deep drilling. There are five main types of hydrothermal alteration in the Sulphur district: (1) propylitic, (2) interstratified illite-smectite and illite, (3) opal-K feldspar, (4) montmorillonite + mordenite (zeolite), and (5) acid sulfate. Brief descriptions of propylitic, opal-K feldspar, illite-smectite, and montmorillonite + mordenite alteration, followed by a detailed description of acid sulfate alteration, are given below.

Propylitic alteration

Propylitic alteration occurs in the Kamma Mountains group, mainly lateral to, and locally within, zones of illite-smectite or illite alteration. The extent and distribution of

propylitic alteration is poorly defined. The mineralogy of the propylitic zone is quartz + K feldspar + chlorite + calcite + illite + marcasite + pyrite ± leucoxene ± siderite.

Opal-K feldspar alteration

Opal-K feldspar alteration covers a large near-surface area (Fig. 4), ranging from about 60 to 213 m thick. This alteration is characterized by intense silicification consisting of opal and chalcedony, with between 15 and 50 percent K feldspar and minor amounts of marcasite + pyrite ± stibnite ± leucoxene and/or rutile. Potassium feldspar in this zone replaces volcanic clasts and fine particles in the matrix and is extremely fine-grained, with individual crystals less than $0.1 \mu\text{m}$ in size. Opal-K feldspar alteration contains pervasive low-grade Au-

Ag values. Minor veins of banded chalcedony \pm calcite occur within opal-K feldspar alteration.

A black to dark brown, opaque (some thin edges are reddish-brown to dark brown) bitumen, with low reflectance (less than quartz or calcite) and blue fluorescence occurs in opal-K feldspar alteration and quartz and calcite veins. The term "bitumen" is here used to describe solid or liquid organic material that has migrated from its source to form solid hydrocarbon (Parnell, 1993). Bitumen is generally not visible macroscopically, although a few crustiform-colloform banded chalcedony veins contain dark bitumen-rich bands that are clearly visible in hand samples. Vein samples from near the present surface to over 425 m in depth contain trace amounts to over 10 percent bitumen, averaging between 2 and 4 percent bitumen. Bitumen typically occurs as disseminations in chalcedony, opal, quartz, or calcite, as vug fillings, and locally as discrete bitumen-rich bands in colloform or crustiform banded veins. A sample of coarse-grained, dark brown to black calcite contains an estimated 20 percent bitumen along cleavage surfaces and disseminated within calcite rhombs and most likely gets its color from the abundance of bitumen.

Illite-smectite alteration

Below the near-surface opal-K feldspar alteration, the Sulphur group sediments are intensely argillized to interlayered illite-smectite + quartz + pyrite \pm chlorite \pm illite \pm calcite \pm kaolinite \pm pyrrhotite (Fig 4). This illite-smectite alteration is pervasive throughout the sediments and extends more than 600 m below the surface. An envelope of illite alteration (<5% interstratified smectite) + quartz + pyrite \pm chlorite \pm calcite is developed around steeply dipping silicified fault zones. This envelope grades outward away from the fault zone into illite-smectite alteration with increasing smectite composition. Calcite veins and veinlets locally cut the illite-smectite alteration, and small (30–50 μ m) rhombs of calcite are disseminated in the illite-smectite + quartz matrix.

Montmorillonite + mordenite alteration

Montmorillonite + mordenite alteration occurs mainly in the northwest Sulphur district (Fig. 3), where it partially overprints opal-K feldspar alteration and sinter deposits, and also alters unconsolidated or poorly consolidated alluvium. This alteration is restricted to the near surface, typically extending no deeper than 50 m below the base of alluvium. This assemblage is typically oxidized and consists mainly of montmorillonite, the zeolite mordenite $(\text{Na}_2, \text{K}_2, \text{Ca})[\text{Al}_2\text{Si}_{10}\text{O}_{24}] \cdot 7\text{H}_2\text{O}$, and chalcedony or quartz. Lesser, but locally significant, amounts of interlayered kaolinite-smectite and kaolinite are present. Minor amounts of jarosite and alunite occur within narrow fractures cutting mordenite-type alteration, are very fine grained, and appear to be late. Where montmorillonite + mordenite alteration has overprinted earlier opal-K feldspar alteration, marcasite and pyrite have been oxidized.

Acid sulfate alteration

Acid sulfate alteration is a type of intense advanced-argillic alteration containing alunite + kaolinite + quartz (Hemley and Jones, 1964). Acid sulfate alteration is extensive and well preserved at the Crofoot-Lewis mine, and occurs both as a widespread blanket that caps a large portion of the deposit,

termed "blanket acid sulfate alteration," and as steeply dipping veins and zones that extend beneath the blanket zone into the underlying opal-K feldspar alteration, termed "acid sulfate veins" (Figs. 5 and 6B).

Blanket acid sulfate alteration

Blanket acid sulfate alteration is vertically zoned, with an upper zone of intensely leached material consisting of residual quartz and cristobalite, termed "blanket acid leach," and a thin lower zone of intense opalization, termed "basal acid leach" (Fig. 5). Blanket acid leach varies in thickness from zero to 100 m and consists mainly of a barren, bleached white, skeletal residue of white powdery quartz + cristobalite, with lesser amounts of opal-A, alunite, natroalunite, kaolinite, native sulfur, gypsum, cinnabar, and jarosite (Fig. 6C). This zone is poorly consolidated and has a high porosity; however, despite the intense leaching, original rock textures are well preserved in many areas. The intensity of acid sulfate alteration generally increases toward major faults and extends to greater depths along some of these structures. Scattered remnants of unleached opal-K feldspar alteration occur within blanket acid leach (Fig. 5), indicating that blanket acid leach alteration has overprinted opal-K feldspar alteration. An interval of hematite-stained alluvium, ranging from a few centimeters to 7 m in thickness, is common at the interface of acid leach alteration and overlying alluvium.

With the exception of cinnabar, sulfides do not occur within blanket acid sulfate alteration. Cinnabar coats native sulfur crystals or occurs disseminated in intense acid-leached material. Native sulfur occurs in beds, lenses, and fracture fillings within the blanket acid leach zone, and in some areas, native sulfur fills open space fractures along fault zones below this zone. Small horizontal beds and oval-shaped elongate pods of fine-grained alunite + kaolinite + silica \pm montmorillonite occur locally in the upper part of the blanket acid leach zone (Fig. 5). These appear to be remnant mud pools which are common at the surface in areas of steam-heated acid sulfate springs in geothermal systems (e.g., Waiotapu, New Zealand; Hedenquist and Browne, 1989). Remnant mud pools are especially abundant in the upper portion of the Boneyard pit where they occur as horizontal beds and lenses of fine-grained alunite + kaolinite + opal-C + opal-CT \pm montmorillonite up to 0.9 m thick and 15 m in length (Fig. 6D). These beds are typically surrounded above, below, and laterally by opalized or kaolinized hydrothermal eruption breccia.

Basal acid leach alteration

Basal acid leach alteration occurs as a subhorizontal unit at the base of blanket acid leach alteration (Fig. 5). Basal acid leach alteration ranges from less than 1 m to over 12 m thick and commonly contains traces to ore-grade Au (averaging up to 0.6 g/t) and relatively little Ag. Basal acid leach alteration has overprinted earlier opal-K feldspar alteration, as evidenced by remnant patches of opal-K feldspar alteration within this zone. Basal acid leach alteration is characterized by dense opalization, normally white or gray in color, but may be a variety of colors including red where hematite is abundant in the matrix (Fig. 6G). Typically, both matrix and clasts are altered completely to opal-A, opal-CT, or chalcedony, with the original breccia or conglomerate textures pre-

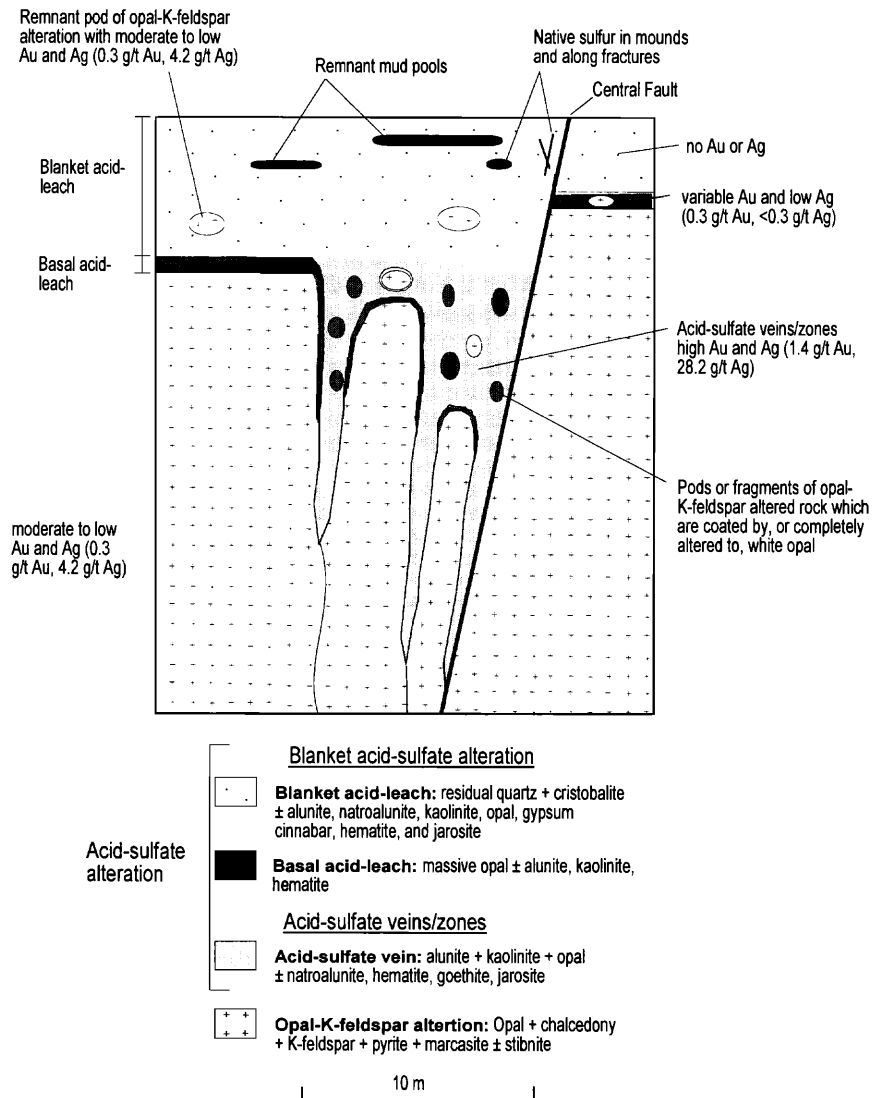


FIG. 5. Schematic vertical section through the upper alteration zones at the Crofoot-Lewis mine, illustrating the vertical zonation and precious metal distribution within acid sulfate alteration. Average Au-Ag grades in parenthesis.

served. Locally, alunite + kaolinite ± hematite are dominant in the matrix. Basal acid leach alteration, although widespread, is not always present and is typically poorly developed or absent in the highly fractured rocks overlying zones of mineralized acid sulfate veins (Fig. 5).

Acid sulfate veins

At the base of the blanket acid sulfate alteration, steeply dipping veins and zones of opal + alunite + kaolinite + montmorillonite ± natroalunite ± hematite ± goethite ± jarosite ± antimony oxides ± pyrite (at depth) fill open-space fractures and brecciated zones in the underlying opal-K feldspar alteration. There is a continuous transition from the blanket acid leach zone (and basal acid leach zone where developed) to the underlying acid sulfate veins, since the veins extend from the base of the blanket acid leach zone but do not cut it (Fig. 5). Acid sulfate veins as thick as 2.4 m exist, but most range from a few millimeters to about 0.5

m, and all of the veins narrow with depth. Most acid sulfate veins do not extend more than 100 m below the base of the blanket acid leach zone, although a few veins extend more than 200 m below this zone. These veins show a crude spatial and temporal zoning from early opal (commonly opal-CT) to alunite + kaolinite to late montmorillonite. Veins with white opal selvages and alunite + kaolinite interiors occur locally (Fig. 5). In pervasive zones of acid sulfate alteration, white opal commonly coats fragments that are surrounded by alunite + kaolinite ± montmorillonite, and late veins of pink montmorillonite locally cut these zones. In places, acid sulfate veins fill the center of earlier formed quartz or chalcedony veins.

At deeper levels (>70 m depth) some of the acid sulfate veins contain fine-grained pyrite and locally traces of marcasite. The pyrite is very fine grained (<0.1 mm) or occurs as small cubes that are disseminated or form bands within or adjacent to alunite, natroalunite, opal, and/or quartz, and ka-

olinite. Several of these pyrites have anomalous As, Ni, and locally, Co.

Some steeply dipping acid sulfate veins contain sections with preserved horizontal beds and laminations of very fine grained mixtures of opal + alunite + kaolinite (Fig. 6E). Some of these horizontal laminations contain structures indicative of soft sediment deformation, as wall-rock fragments have fallen into veins and deformed the laminations (Fig. 6F). These textures indicate that the veins formed as open-space fillings and were filled from the bottom up. This suggests that much of the opal + alunite + kaolinite \pm montmorillonite in these veins precipitated from solution. However, alteration of preexisting minerals such as feldspars to alunite or kaolinite is apparent in the vein selvages and in partially overprinted pods of opal-K feldspar alteration that occur within blanket acid leach alteration, basal acid leach alteration, and mineralized acid sulfate veins or zones.

Alunite from the blanket acid leach zone and the acid sulfate veins is typically white and generally very fine grained; in some of the deeper acid sulfate veins, alunite has a light pink color. Alunite crystals are lath or rhomb shaped, or less commonly, cubic or anhedral. Most alunite samples contain grains that range in size from <1 to about $20 \mu\text{m}$; however, the majority of grains are approximately the same size. Within the blanket acid leach zone, alunite laths and rhombs range from 1 to $18 \mu\text{m}$ in length, averaging $5 \mu\text{m}$. In the acid sulfate veins, alunite ranges from less than 1 to $15 \mu\text{m}$ in length, and the deepest vein sample is also the coarsest. Associated kaolinite crystals are typically very fine grained, predominantly $1 \mu\text{m}$ or less. Scanning electron microscope analyses reveal that several pure alunites (K end member) and natroalunites (Na end member) occur. However, many alunites contain significant amounts of Na, and many natroalunites contain significant amounts of K. Most alunites and natroalunites contain no detectable Fe or Ca, although, in a few of the deeper acid sulfate veins, alunite or natroalunite is enriched in Ca at the expense of K or Na.

Mineralization

Introduction

Several zones of economic mineralization have been defined at the Crofoot-Lewis mine, including the Bay area, Lewis pit, South Extension pit, Gap pit, South Central pit, Boneyard pit, and Brimstone pit (Fig. 3). Mineralization is hosted dominantly by Camel conglomerate, Crofoot breccia, and Kamma Mountains group volcanic rocks. Unoxidized, mineralized, opal-K feldspar alteration extends over a large area and constitutes a huge Au-Ag resource ($>116,000$ kg Au; Ebert, 1995), but is uneconomic due to its low-grade (0.27 g/t Au and 4.15 g/t Ag) and refractory nature. Higher grades occur within this unit, and the Bay area contains a refractory resource of about 7 Mt at a grade of 1.20 g/t Au. Economic near-surface Au-Ag mineralization occurs in four styles (Ebert et al., 1996); horizontally controlled near-surface ore, mineralized acid sulfate alteration, mineralized basal acid leach, and late quartz-chalcedony veins.

Horizontally controlled near-surface ore

The majority of ore in the Bay area came from mineralized opal-K feldspar alteration and interbedded sinter that was

overprinted, and oxidized, by near-surface montmorillonite-mordenite alteration. Oxidation of this ore style is independent of structure, and locally is bedding controlled and is referred to as "horizontally controlled." Oxidized ore in this zone contains comparable grades as the underlying unoxidized mineralized opal-K feldspar alteration, and there are no indications of precious metal remobilization or enrichment.

Mineralized acid sulfate alteration

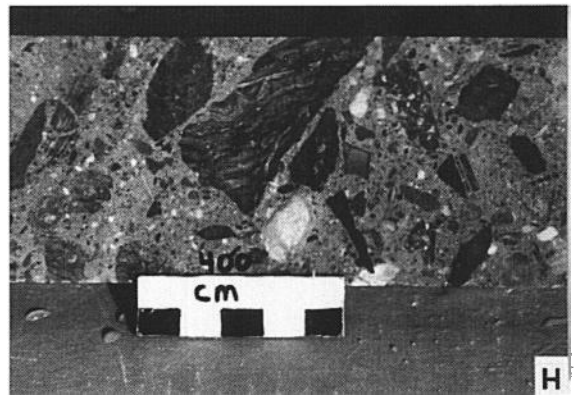
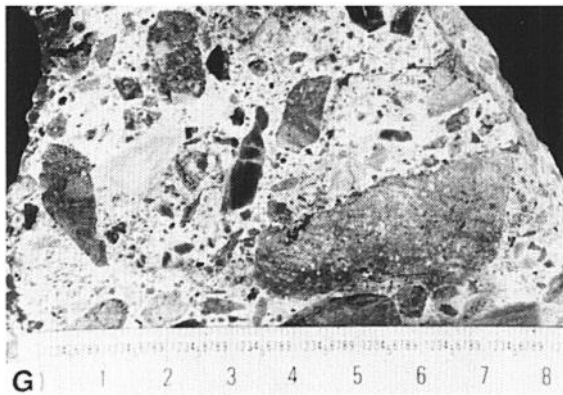
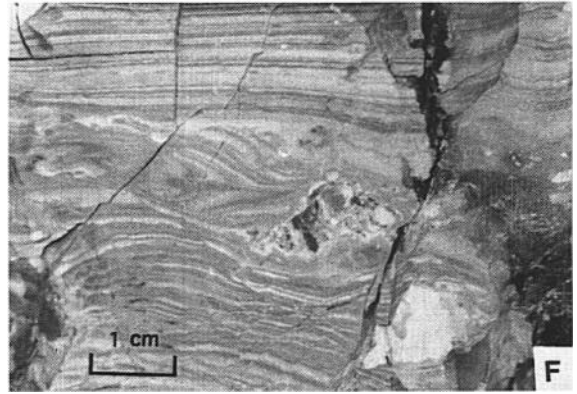
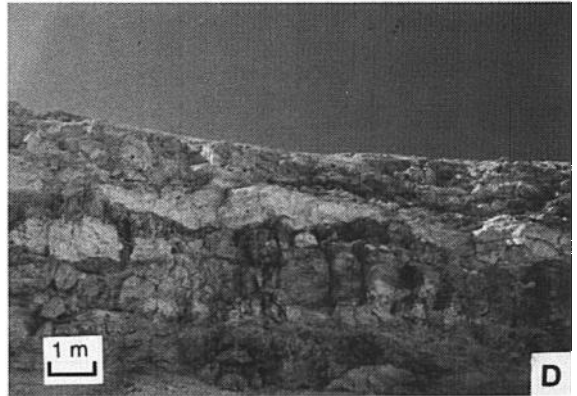
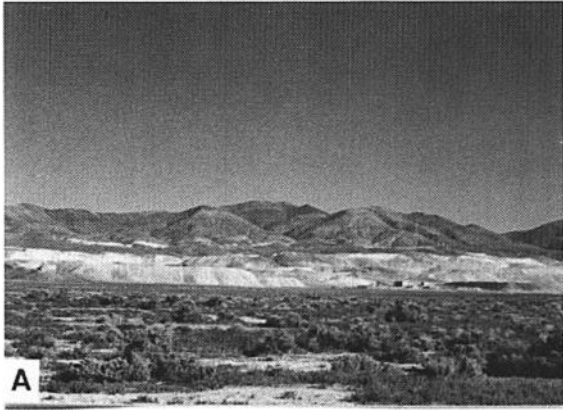
The majority of ore mined to date consists of steeply dipping acid sulfate veins and zones that fill open-space fractures below the blanket acid leach zone (Figs. 5 and 7). The Lewis, Gap, South Central, and Brimstone pits are examples of this type of mineralization. Areas of mineralized acid sulfate alteration have formed within opal-K feldspar alteration that has been intensely fractured, predominantly in the hanging wall of the Central fault within a well-defined graben structure, where ore is continuous for at least 3 km. Zones of pervasive acid sulfate mineralization consist mainly of white opaline (\pm chalcedony) fragments that are surrounded by alunite + kaolinite + opal-chalcedony + montmorillonite. The white fragments are typically opal coated and/or opalized fragments of earlier opal-K feldspar alteration. Hematite and goethite \pm jarosite give the zone its red and/or yellow hues. Pervasive acid sulfate mineralization gives way at depth to narrow, steeply dipping, mineralized acid sulfate veins.

Figure 7 shows a wall from the south face of the South Central pit and is an example of the mineralized acid sulfate alteration currently being mined at the deposit. In this area the bulk of the orebody consists of numerous, steeply dipping, mineralized acid sulfate veins which are widely spaced but have relatively high grades, making them bulk mineable. Individual acid sulfate veins have values up to 63 g/t Au, with an average grade (20 vein samples) of 6.4 g/t Au. The Ag contents of these veins reach values over 157 g/t and are typically several times higher than the Au content. Adjacent unoxidized opal-K feldspar alteration averages only 0.27 g/t Au and 3.43 g/t Ag through this section, indicating that the acid sulfate veins are substantially enriched in Au and Ag relative to the surrounding opal-K feldspar altered rock. The zone as a whole has an average grade of 0.89 g/t Au. In individual acid sulfate veins, the Au-Ag content is highest near the top and decreases with depth.

Scanning electron microscope analyses shows that Au in these zones occurs as micron-size electrum grains, within and adjacent to opal, alunite, kaolinite, or montmorillonite. Most of the electrum associated with acid sulfate mineralization has between 27 and 35 percent Ag, averaging 31 percent Ag. Silver also occurs as cerargyrite (AgCl) and less commonly iodargyrite (AgI) associated with alunite, kaolinite, or jarosite.

Mineralized basal acid leach

A thickened portion of mineralized basal acid leach hosts ore in the Boneyard pit. This ore is characterized by Crofoot breccia in which both clasts and matrix have been altered to white opal + alunite + kaolinite \pm hematite. Textures and remnants of mineralized opal-K feldspar alteration indicate mineralized basal acid leach has overprinted, and altered, mineralized opal-K feldspar alteration. mineralized basal acid leach accounts for a small portion of the ore at the Crofoot-



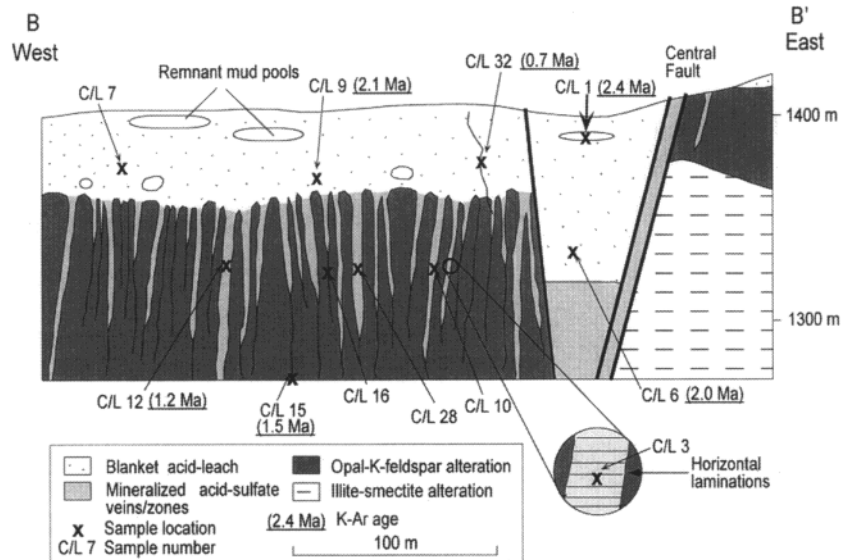


FIG. 7. Simplified east-west cross section through the South Central pit showing alteration, sample locations, and K-Ar ages. An enlargement of an acid sulfate vein containing horizontal laminations is also shown. Rock types (not shown) consist dominantly of conglomerates and breccias.

Lewis mine, consisting of 2,250,000 t grading 0.55 g/t Au, with relatively low Ag values.

Late quartz-chalcedony veins

Mineralized quartz \pm chalcedony veins and veinlets cut and infiltrate blanket acid leach alteration, opal-K feldspar alteration, and illite + quartz + pyrite alteration in the Brimstone area. These veinlets create localized zones of ore-grade mineralization within the blanket acid leach zone, a feature unique to the Brimstone area. Mineralization within the blanket acid leach zone could account for up to half of the economic mineralization within the Brimstone pit, which contains about 39 Mt at a grade of 0.58 g/t Au. A mineralized stockwork containing similar veinlets occurs beneath the Brimstone pit; however, its distribution and extent is poorly defined.

Age of Mineralization

Age of opal-K feldspar and illite-smectite alteration

Until recently the age of opal-K feldspar and illite-smectite alteration at the Crofoot-Lewis mine was enigmatic. Unpublished K-Ar ages of K feldspar obtained from opal-K feldspar altered breccia gave dates ranging from Early to Late Miocene (samples C/L 74, 75, and 76; D. John and T. McKee,

pers. commun., 1994) and were difficult to reconcile with the geology of the deposit and the timing of acid sulfate alteration. Potassium-Ar and ^{40}Ar - ^{39}Ar age data are summarized in Table 1.

Examination of opal-K feldspar altered breccia by scanning electron microscope revealed that K feldspar in the breccia matrix is stoichiometric whereas K feldspar replacing the volcanic breccia clasts contains significant amounts of CaO and Na₂O which increase toward the center of the clasts. Presumably, the presence of CaO and Na₂O in K feldspar within the volcanic clasts is a result of incomplete replacement of magmatic feldspar by hydrothermal K feldspar, and this incomplete replacement may account for the older than expected K-Ar ages obtained from the breccia samples (Ebert, 1995).

To resolve the dilemma, laser probe $^{40}\text{Ar}/^{39}\text{Ar}$ dating of hydrothermal K feldspar within the matrix and within clasts of opal-K feldspar altered breccias was performed. K feldspar in the breccia matrix yielded $^{40}\text{Ar}/^{39}\text{Ar}$ ages of 3.8 ± 0.09 and 3.9 ± 0.3 Ma (samples C/L 77 and C/L 78), whereas K feldspar in the volcanic clasts yielded ages of 10.6 ± 0.17 and 14.9 ± 1.6 Ma (samples C/L 79 and C/L 81). The ages obtained from the matrix are interpreted to represent the age of opal-K feldspar alteration whereas the older ages obtained

FIG. 6. A. View of the Crofoot-Lewis deposit from the valley floor, facing east toward the pediment and range. B. View of the south wall of the South Central pit facing southwest. Blanket acid leach alteration (light color) occurs like a blanket above the ore zone (darker colored) that extends below the base of the pit. The benches are 6 m high. The Silver Camel hill, a partially exposed silicified fault zone forms the ridge in the background. C. Blanket acid leach alteration, southeast wall of southern most extension of the South Central pit. Benches are 6 m high. D. Close up of blanket acid leach alteration containing horizontal pods composed of fine-grained alunite + silica + kaolinite, interpreted as fossilized mud pools. E. Horizontal beds and laminations composed of alunite + silica + kaolinite from a large vertical acid sulfate vein. South Central pit. F. Close up of horizontal laminations within a near-vertical acid sulfate vein. Note the soft sediment-type deformation created by the two wall-rock fragments (right center) that appear to have fallen into the vein. G. Basal acid leach-altered breccia. The matrix and clasts are dominantly massive opal with minor alunite and kaolinite. The clasts appear darker due to the presence of hematite. H. Opal-K feldspar altered hydrothermal eruption breccia.

TABLE 1. K-Ar and ^{40}Ar - ^{39}Ar Age Data for the Crofoot-Lewis Deposit

Sample no.	Mineral	Description	K-Ar age (Ma)	^{40}Ar - ^{39}Ar age (Ma)
C/L 1	Alunite	Blanket acid leach zone	2.4 ± 0.1^1	
C/L 2	Alunite	Acid sulfate vein	0.9 ± 0.6^1	
C/L 6	Alunite	Blanket acid leach zone	2.0 ± 0.1^1	
C/L 9	Alunite	Blanket acid leach zone	2.1 ± 0.1^1	
C/L 12	Alunite	Acid sulfate vein	1.2 ± 0.13^1	
C/L 15	Alunite	Acid sulfate vein	1.5 ± 0.12^1	
C/L 32	Jarosite	Fracture filling in blanket acid leach zone	0.7 ± 0.2^2	
C/L 71	Illite	Illite + quartz + pyrite altered volcanic rock	4.0 ± 0.2^1	
C/L 74	K feldspar	Oxidized opal-K feldspar breccia	9.3 ± 0.3^1	
C/L 75	K feldspar	Oxidized opal-K feldspar breccia	23^1	
C/L 76	K feldspar	Unoxidized opal-K feldspar breccia	10.3 ± 0.3^1	
C/L 77	K feldspar	Breccia matrix		3.8 ± 0.09^2
C/L 78	K feldspar	Breccia matrix		3.9 ± 0.3^2
C/L 79	K feldspar	Felsic volcanic breccia clast		10.6 ± 0.17^2
C/L 81	K feldspar	Felsic volcanic breccia clast		14.9 ± 1.6^2

¹ D. John and E. McKee, U.S. Geological Survey, Menlo Park, California (unpublished data)

² I. Kigai and M. Karpenko, Institute of Geology and Ore Deposits, Petrography, Mineralogy, and Geochemistry, Russian Academy of Sciences, Moscow (unpublished data)

from the volcanic clasts are thought to be somewhere between the age of hydrothermal alteration and the age of the volcanic clasts. Temperatures in this near-surface environment appear to have been insufficient to reset older K feldspar. An illite sample (C/L 71) separated from an intensely illite + quartz + pyrite altered zone gave a K-Ar age of 4.0 which is concordant with the $^{40}\text{Ar}/^{39}\text{Ar}$ ages of the K feldspar matrix.

Age of acid sulfate alteration

Alunite K-Ar ages vary between 2.4 and 0.9 Ma (Table 1); the location of several alunites and the jarosite from the blanket acid leach zone and underlying acid sulfate veins along with available K-Ar ages are shown in Figure 7. In Figure 7 alunites from the blanket zone give older ages than alunites from the underlying veins. Field relations (Fig. 7) show that the veins do not crosscut the overlying blanket zone but simply extend downward from its base. This relation, combined with stable isotope data discussed below, and precious metal distribution, suggests that the blanket acid leach zone is likely to be the same age as the underlying veins and not older, as the K-Ar ages indicate. Given the uncertainty of the analyses these samples could all be about the same age.

Coarse-grained (up to 4 mm) jarosite (sample C/L 32) from narrow fractures cutting the blanket acid leach zone yielded a K-Ar age of 0.7 ± 0.2 Ma. This coarse-grained sample has isotopic compositions characteristic of a steam-heated origin and represents the youngest documented episode of geothermal activity.

Field Evidence for a Steam-Heated Origin for Acid Sulfate Alteration

Acid sulfate alteration commonly forms in four geologically distinct environments: supergene, steam-heated, magmatic

hydrothermal, and magmatic steam (Rye et al., 1992). In the supergene environment acid sulfate alteration results from the acid waters that form by the weathering of sulfide-bearing rocks that are exposed above the water table (e.g., Guilbert and Park, 1986). In the steam-heated environment, acid solutions form by the oxidation of H_2S to sulfate in the vadose zone; in this environment H_2S is derived from boiling liquid at depth (e.g., Schoen et al., 1974). In some cases this H_2S may be associated with bursts of magmatic steam (e.g., the Cactus, CA, deposit, Rye et al., 1992). The end products of supergene and steam-heated acid sulfate alteration zones can be similar, but the distinction between the two can be made by isotope studies in the context of time-space frameworks (Rye et al., 1992). Magmatic-hydrothermal acid sulfate alteration is associated with high-sulfidation-type ore deposits and is formed in hydrothermal systems with acid magmatic components in their fluids (Rye et al., 1992). In this environment extremely acid conditions are formed by the disproportionation of magmatic SO_2 and the presence of HCl and other acids, subsequent to magmatic vapors being absorbed by ground water (e.g., Holland, 1965; Henley and McNabb, 1978; Stoffregen, 1987; Hedenquist et al., 1994). The magmatic steam environment is characterized by the formation of veins of almost pure coarse-banded alunite in extensional faults. The alunites are believed to form from the oxidation of the SO_2 -rich magmatic fluids by the loss of hydrogen or the entrainment of atmospheric oxygen. The dominance of SO_2 in the fluids is believed to result from the decompression of magmatic fluids (Rye, 1993).

Field evidence indicates that the blanket acid leach zone at the Crofoot-Lewis deposit formed in a steam-heated environment. Here acid sulfate alteration occurs dominantly as a horizontal blanket that caps the system, generally lacks sulfides, and is zoned vertically, from a leached residual cap (blanket acid leach) at the top, to a narrow interval of intense opalization (basal acid leach). The lower zone of acid sulfate alteration is inferred to coincide with the paleowater table (e.g., Schoen et al., 1974). The deepest extent of acid alteration consists of underlying veins of opal-chalcedony + alunite + kaolinite \pm montmorillonite (Fig. 5). This zonation is common in steam-heated acid sulfate alteration zones in active geothermal systems such as Steamboat Springs, Nevada (Schoen et al., 1974), Roosevelt Hot Springs, Utah (Parry et al., 1980), and in the Norris Geyser basin at Yellowstone Park, Wyoming (White et al., 1988). Within the blanket acid leach zone, the presence of native sulfur, remnant mud pools similar to those that occur in geothermal systems, and the association with cinnabar indicate that this alteration formed in a steam-heated environment. In numerous localities at the Crofoot-Lewis mine bedded mounds and lenses of native sulfur contain vertical, elongate vesicles, a texture that indicates the sulfur was molten, and therefore, had a minimum temperature around 113° to 120°C (White et al., 1988). Combined, these textures and temperatures preclude supergene processes.

The presence of magmatic hydrothermal, acid sulfate alteration can be ruled out based on the geometry of the acid sulfate alteration, the general absence of sulfide minerals in this zone, and as discussed below, the lack of a detectable magmatic component (e.g., Rye et al., 1992). Stable isotope

data, presented below, support a steam-heated origin for acid sulfate alteration at the Crofoot-Lewis deposit; however, minor amounts of supergene alunite probably occur in the district.

Evidence for Fluctuations in the Water Table

The level of the water table has a major control on the distribution of epithermal mineralization and alteration assemblages in the near-surface environment (e.g., Foley et al., 1989; Simmons, 1991). At the Crofoot-Lewis deposit alteration assemblages and sinter beds have been used to constrain the level of the water table during the formation of the deposit (Ebert, 1995). The presence of remnant opal-K feldspar alteration (an assemblage that forms below the water table; Browne, 1978; Henneberger and Browne, 1988) within blanket acid sulfate alteration (an assemblage that forms above the water table; Schoen et al., 1974) demonstrates that the water table dropped between the period of early opal-K feldspar alteration and later acid sulfate alteration. Overprinting of opal-K feldspar alteration by blanket acid sulfate alteration indicates that the water table dropped a minimum of 18 m during acid sulfate alteration.

Mineralized stockwork quartz veining has been exposed in recent mining excavations and encountered in two core holes in the proposed Brimstone pit. This stockwork cuts blanket acid sulfate alteration in the Brimstone area. The distribution and extent of this stockwork is poorly constrained; however, the core samples demonstrate that late crosscutting quartz veining extends a minimum of 50 m above the base of the blanket acid sulfate zone (Ebert, 1995). This requires at least a 50-m rise in the level of the water table following acid sulfate alteration.

Shallow Enrichment Processes for Precious Metals

Figure 5 illustrates the relationship between relatively high-grade oxidized acid sulfate mineralization, relatively low-grade unoxidized opal-K feldspar mineralization, and barren blanket acid leach alteration. The presence of remnant patches of weakly mineralized opal-K feldspar alteration within barren blanket acid leach alteration is evidence that blanket acid leach alteration overprinted weakly mineralized opal-K feldspar alteration and removed Au and Ag. The mineralized acid sulfate veins and zones locally contain several times more Au and Ag than adjacent opal-K feldspar alteration, and simple mass-balance calculations demonstrate that leaching of Au from the overlying blanket acid-leached material can account for most of the observed Au increase in the underlying acid sulfate ore (Ebert, 1995; Ebert et al., 1996). We propose that a dropping water table enabled acid sulfate waters to overprint weakly mineralized opal-K feldspar alteration, resulting in the leaching of Au and Ag as these fluids percolated downward toward the water table. These acid sulfate fluids precipitated Au and Ag (dominantly as electrum, AgCl, and AgI), associated with opal + alunite + kaolinite + montmorillonite, in open-space fractures at, and mainly within a few tens of meters below, the water table. This process resulted in leaching of precious metals from a large area and concentration into relatively confined zones below the water table; they probably formed in a similar manner to classical supergene enrichment zones, the main difference

being that the acid fluids were generated by the oxidation of H₂S gas and not sulfide minerals. The mechanism by which Au and Ag are transported in these acid, relatively oxidizing, low-temperature fluids is uncertain. The ability of the acid sulfate fluids to leach even relatively insoluble elements is displayed by the large areas containing 90 to 100 percent residual silica that have had essentially all other major and minor elements removed (Ebert, 1995). We speculate that thiosulfate and Cl are likely ligands in this environment (e.g., Listova et al., 1968; Mann, 1984; Webster and Mann, 1984; Stoffregen, 1986; Webster, 1986, 1987); however, supporting experimental data are needed. The physical-chemical environment in the steam-heated environment is highly variable and deposition of Au and Ag minerals from such fluids could be triggered by changing f_{O_2} , temperature, evaporation, or mixing.

Stable Isotope Study

Sample descriptions and analytical results

Brief sample descriptions and stable isotope data are summarized in Table 2. Sample locations for several of the samples are shown in Figure 7. The seven kaolinite samples listed in Table 2 were separated from mixtures of fine-grained alunite + kaolinite + silica and are assumed to have formed contemporaneously with the alunite. Six samples of pyrite-marcasite were separated from samples of opal-K feldspar alteration, and one sample of pyrite was separated from a sample of illite-smectite alteration. In addition, two pyrite samples (samples C/L 13 and C/L 17) were separated from narrow alunite-kaolinite-pyrite veins that occur relatively deep in the system. A whole-rock $\delta^{34}S$ value was obtained from an unaltered felsic volcanic rock from the Kamma Mountains group (sample C/L 58) and a $\delta^{34}S$ value of pyrite was obtained from interlaminated slate and metasilstone from the Auld Lang Syne Group (sample C/L 43).

Three samples of present-day surface and subsurface acidic waters have been analyzed for aqueous sulfur. The subsurface acid water was sampled in an area which contains no oxidized rock and most likely originated by oxidation (at shallow depths) of H₂S gas that is presently exsolving from a reservoir of warm water at depth. Exploration drill holes have encountered warm (up to 40°C), locally acidic (pH to 3.9) water and H₂S gas. Standard stable isotope techniques were used and are summarized in Ebert (1995).

Discussion of Isotopic Data

Oxygen and hydrogen isotope data for alunite, jarosite, and kaolinite

Figure 8 shows the fields for the possible compositions of supergene alunite and kaolinite (Rye et al., 1992). The shaded region labeled SASF is the field for δD - $\delta^{18}O_{SO_4}$ values for supergene alunite in the absence of bacterial reduction of aqueous sulfate or exchange of aqueous sulfate with low pH waters. The area between the dotted lines labeled SAOZ represents the possible range of δD - $\delta^{18}O_{OH}$ values in supergene equilibrium with meteoric water between 20° and 80°C. These fields are for reference only and many nonsupergene alunites have isotopic compositions within both of these fields (Rye et al., 1992). Most of the alunites in Figure 8 cluster in

TABLE 2. Summary of Isotopic Data on Minerals from the Crofoot-Lewis Deposit, Sulphur, Nevada

Sample no.	Location	Mineral	Description	Avg grain size (μm)	δD (SMOW, ‰)	$\delta^{18}\text{O}_{\text{SO}_4}$ (SMOW, ‰)	$\delta^{18}\text{O}_{\text{OH}}$ (SMOW, ‰)	$\delta^{34}\text{S}$ (CDT, ‰)	$\delta^{18}\text{O}$ (SMOW, ‰)	Temperature ¹ (°C)
C/L 1	S-C pit	Alumite	Blanket zone	5	-162	4.2	-5	-7.4		40
C/L 2	Lewis pit	Alumite	Acid sulfate vein	1	-120	-3	5.6	-14		
C/L 3	S-C pit	Alumite	Acid sulfate vein	3	-128	6.8	-4	-5.3		90
C/L 3	S-C pit	Quartz	Acid sulfate vein						5.5	
C/L 4	Boneyard pit	Alumite	Blanket zone	2.5	-111	4.9	2.3	-9.3		440
C/L 4	Boneyard pit	Alumite	Mud pool, blanket zone	2.5	-111	2.4	1.8	-10		
C/L 5	Boneyard pit	Alumite	Mud pool, blanket zone	1	-116	7.6	-6	-7.4		60
C/L 5	Boneyard pit	Kaolinite	Mud pool, blanket zone		-157				2.6	
C/L 6	S-C pit	Alumite	Blanket zone	8.5	-107	9.8	1.1	-6.5		50
C/L 7	S-C pit	Alumite	Blanket zone	3	-113	8.9	6.0	-8		380
C/L 8	Brimstone	Alumite	Blanket zone	7	-138	-4.4	-6.6	-11		530
C/L 9	S-C pit	Alumite	Blanket zone	15	-122	7.2	.1	-6.4		90
C/L 10	S-C pit	Alumite	Acid sulfate vein	2.5	-125	2.8	1.1	-5.7		770
C/L 11	Lewis pit	Alumite	Acid sulfate vein	3	-111	.7	9.5	-9.9		180
C/L 12	S-C area	Alumite	Acid sulfate vein	2	-112	3.3	-1.6	-6		20
C/L 13	S-C area	Alumite	Acid sulfate vein	15	-120	9.6	-5	-7.1		
C/L 13	S-C area	Kaolinite	Acid sulfate vein		-169				3.8	
C/L 13	S-C area	Pyrite	Acid sulfate vein					-26		
C/L 14	S-C area	Alumite	Acid sulfate vein	2.5	-124	8.3	.1	-6.6		60
C/L 15	S-C area	Alumite	Acid sulfate vein	5	-125	1.9	-1.7	-7.5		290
C/L 16	S-C pit	Alumite	Acid sulfate vein	3	-120	6.6	.0	-5.5		110
C/L 17	S-C area	Alumite	Acid sulfate vein	15	-119	.4	5.0	-12		
C/L 17	S-C area	Pyrite	Acid sulfate vein					-15		
C/L 18	S-C pit	Alumite	Acid sulfate vein	3	-115	4.0	1.1	-10		380
C/L 18	S-C pit	Kaolinite	Acid sulfate vein		-165				0.2	
C/L 19	S-C pit	Alumite	Acid sulfate vein							
C/L 20	S-C area	Alumite	Acid sulfate vein	3	-136			-4.6		
C/L 20	S-C area	Quartz	Acid sulfate vein						4.7	
C/L 21	S-C pit	Alumite	Acid sulfate vein							
C/L 22	S-C pit	Alumite	Acid sulfate vein	7.5						
C/L 22	S-C pit	Kaolinite	Acid sulfate vein							
C/L 23	Silver Camel	Alumite	Acid sulfate vein-matrix	7.5	-160					
C/L 24	S-C area	Alumite	Acid sulfate vein		-118			-6.2		
C/L 25	S-C area	Alumite	Acid sulfate vein		-147			-2.2		
C/L 25	S-C area	Alumite	Acid sulfate vein		-93			-5.2		
C/L 26	S-C area	Kaolinite	Blanket zone		-145				5.4	
C/L 27	Boneyard pit	Kaolinite	Mud pool, blanket zone		-157				6.1	
C/L 28	S-C pit	Kaolinite	Acid sulfate vein		-166				6.8	
C/L 29	Brimstone	Kaolinite	Blanket zone		-170					
C/L 30	S-C pit	Kaolinite	Acid sulfate vein		-165				2.1	
C/L 31	Lewis pit	Kaolinite	Blanket zone		-166				1.6	
C/L 32	S-C pit	Jarosite	Blanket zone	2,000	-183					70, 87 ²
C/L 32	S-C pit	Quartz	Blanket zone			13.6				
C/L 33	N. Lewis pit	Jarosite	Fracture coating	7	-145	.5	.3	-11		

C/L 34	S. Lewis pit	Jarosite			5	-164	-0.5	-1.2	-13	
C/L 35	S-C area	Pyrite	Fracture coating						-14	
C/L 36	S-C pit	Pyrite	Acid sulfate vein						-11	
C/L 37	S-C pit	Pyrite	Opal-K feldspar alteration						-11	
C/L 38	S-C pit	Pyrite	Opal-K feldspar alteration						-14	
C/L 39	S-C area	Pyrite	Opal-K feldspar alteration						-14	
C/L 40	Lewis pit	Pyrite	Opal-K feldspar alteration						-15	
C/L 41	S-C pit	Pyrite	Opal-K feldspar alteration						-11	
C/L 42	S-C area	Pyrite	Illite-smectite alteration						-15	
C/L 43		Pyrite	Auld Lang Syne Group						-1.9	
C/L 44	Brimstone	Quartz	Late quartz vein in blanket zone						4.1	
C/L 45	S-C area	Quartz	Quartz vein						3.6	125 ²
C/L 46	S-C area	Quartz	Quartz vein			-116			5.5	
C/L 46	S-C area	Fluid inclusions	Quartz vein							125 ²
C/L 47	S-C area	Quartz	Quartz vein			-117			4.7	
C/L 47	S-C area	Fluid inclusions	Quartz vein							19.3
C/L 48	S-C area	Quartz	Quartz vein			-133				
C/L 48	S-C area	Fluid inclusions	Quartz vein							2.6
C/L 49	S-C area	Quartz	Quartz vein			-136				128 ²
C/L 49	S-C area	Fluid inclusions	Quartz vein							
C/L 50	S-C pit	Chalcedony	Opal-K feldspar alteration						5.9	
C/L 51	S-C pit	Chalcedony	Opal-K feldspar alteration						7.5	
C/L 52	S-C area	Chalcedony	Opal-K feldspar alteration						6	
C/L 53	S-C area	Chalcedony	Opal-K feldspar alteration						3.8	
C/L 54	Lewis pit	Chalcedony	Laminated sinter						9.3	
C/L 55	Lewis pit	Acid water	At surface pH = 3.9							
C/L 56	Lewis	Acid water	Subsurface pH = 6.3							
C/L 57	S-C area	Acid water	Subsurface pH = 4.5							
C/L 58	NE of mine	Whole rock	Felsic tuff						10	
C/L 59	Brimstone	Native S	Blanket zone						-9.7 ³	
C/L 60	Brimstone	Native S	Blanket zone						-7.4 ³	
C/L 61	Brimstone	Native S	Blanket zone						-13 ³	
C/L 62	S-C area	Gypsum	Blanket zone						-7 ⁴	
C/L 63	Brimstone	Gypsum	Gypsum replacing calcite						-3.2 ⁴	
C/L 64	Brimstone	Gypsum	Gypsum replacing calcite						-21 ⁴	
C/L 65	Devils Corral	Calcite	Vein in illite-smectite alteration							
C/L 66	Brimstone	Calcite	Large banded calcite vein							
C/L 67	Brimstone	Calcite	Large banded calcite vein							
C/L 68	Devils Corral	Calcite	Vein in illite-smectite alteration							
C/L 68	Devils Corral	Fluid inclusions	Calcite vein			-136			7	125 ²
C/L 69	Brimstone	Calcite	Large banded calcite vein						6.7	98 ²
C/L 69	Brimstone	Fluid inclusions	Large banded calcite vein			-153				
C/L 70	Boneyard pit	Calcite	Quartz-calcite vein						2.7	

Abbreviations: S-C = South-Central; SMOW = standard mean ocean water, CDT = troilite from the Canyon Diablo meteorite

¹ Isotope temperature calculated from fractionation factors of Stoffregen et al. (1994)

² Fluid inclusion homogenization temperature

³ Peter Vlkre, ASARCO Inc., pers. commun. (unpub. data)

⁴ Coastal Science Laboratories James Rueker, pers. commun. (unpub. data)

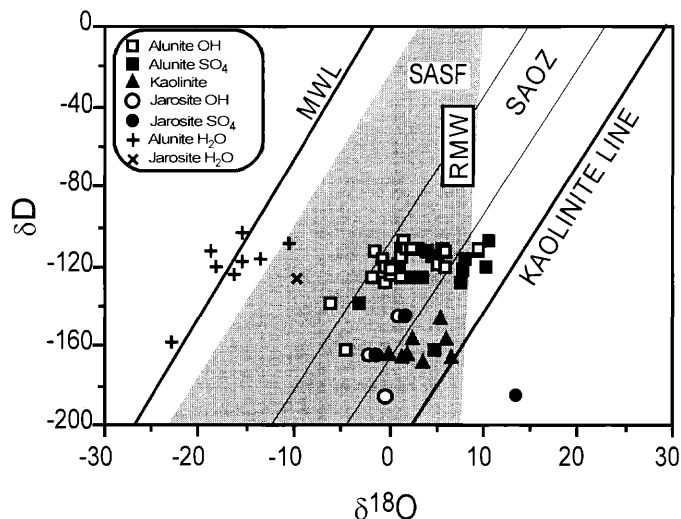


FIG. 8. The δD , $\delta^{18}O_{SO_4}$, $\delta^{18}O_{OH}$ values of alunites and jarosite, δD , and $\delta^{18}O$ of associated kaolinites, and calculated δD_{H_2O} and $\delta^{18}O_{H_2O}$ of fluids for alunites and jarosite sample C/L 32. Fluid compositions calculated from equations of Stoffregen et al. (1994) and Rye and Stoffregen (1995). Lines and fields are MWL = meteoric water line of Craig (1961); PMW = primary magmatic water field of Taylor (1979); kaolinite line of Savin and Epstein (1970); SASF (shaded) = supergene alunite SO_4 field; and SAOZ = supergene alunite OH zone as described in Rye et al. (1992).

a group with δD values around -120 per mil and $\delta^{18}O_{OH}$ and $\delta D - \delta^{18}O_{SO_4}$ values between about 0 and 10 per mil. Two alunites fall outside this group, with δD values near -160 per mil. The δD values for jarosites are much lower than those for alunite, with a range from -183 to -145 per mil. Supergene kaolinites or halloysites typically have δD and $\delta^{18}O$ values close to the kaolinite line (Lawrence and Taylor, 1971; Marumo et al., 1982). The kaolinites all plot to the left of the supergene kaolinite line in a tight group with an average δD of about -160 values and a range of $\delta^{18}O$ values of about 0 to 7 per mil (Fig. 8).

Alunite $\Delta^{18}O_{SO_4-OH}$ temperatures

The $\delta^{18}O_{OH}$ values of alunite are commonly in equilibrium with the parent water, and if the aqueous SO_4 also reached oxygen isotope equilibrium with the parent water, the isotopic data of alunite can be used as a single-mineral isotopic geothermometer (Rye et al., 1992; Stoffregen et al., 1994). The average uncertainty of these temperatures is probably about $\pm 30^\circ C$.

Eight of the alunites from the Crofoot-Lewis mine yield $\Delta^{18}O_{SO_4-OH}$ temperatures that range from 40° to $180^\circ C$, consistent with a steam-heated origin. The $\Delta^{18}O_{SO_4-OH}$ values of the other alunites yield unrealistic temperatures for this shallow environment and are inconsistent with those of the present mineral assemblages. Similar values have been obtained for alunites from the steam-heated zones in active geothermal systems (Rye et al., 1992) and are typical of those of steam-heated alunites in which oxygen isotope equilibrium was not obtained for the aqueous sulfate.

Figure 9 is a plot of depth vs. calculated $\Delta^{18}O_{SO_4-OH}$ temperatures for alunites yielding reasonable formation temperatures from the blanket acid leach zone and the underlying

acid sulfate veins. Four alunites from the blanket acid leach zone give temperatures between 40° and $90^\circ C$. Such temperatures are reasonable for alunites that originate in the zone above the water table, where temperatures will generally not exceed $100^\circ C$ (Rye et al., 1992). Four alunite samples from acid sulfate veins have temperatures that range from 60° to $180^\circ C$. Such higher temperatures for alunites in the acid sulfate veins are consistent with their greater depth in the geothermal system.

Isotopic data of sulfate and sulfides

Figure 10A is a plot showing the $\delta^{18}O_{SO_4}$ vs. $\delta^{34}S$ values of alunite, and the $\delta^{34}S$ ranges for six samples of pyrite and marcasite from opal-K feldspar alteration, and sulfate from three samples of present-day acid water. The $\delta^{34}S$ values for early sulfides range from -10.8 to -15.2 per mil and these values approximate the $\delta^{34}S$ values of H_2S in the geothermal fluid, because fractionation between aqueous H_2S and pyrite is small at the relatively low temperatures ($< 180^\circ C$) likely to have been attained in this alteration zone (Ohmoto and Rye, 1979; Rye et al., 1992). All but two of the alunites are enriched in ^{34}S relative to early sulfides.

The $\delta^{34}S$ value of pyrite sample C/L 42 (-14.5‰) separated from the widespread illite-smectite alteration is within the interpreted $\delta^{34}S$ range of initial H_2S . The source of the S for pyrite in the illite-smectite alteration zone was most likely the H_2S that was exsolved from boiling solutions which flowed along permeable zones and condensed (along with CO_2) into marginal, relatively stagnant, ground water. This source agrees with models for the formation of interstratified illite-smectite alteration by Barton et al. (1977) at Creede, and Hedenquist (1990) at the Broadlands geothermal system, New Zealand.

Figure 10B is a plot of alunite $\delta^{34}S$ vs. $\Delta^{18}O_{SO_4-OH}$ values. All of the alunites from the blanket acid leach zone have partially exchanged $\delta^{34}S$ values, and these values overlap with, but have a wider range than, those of the blanket alunites. Most of the alunites with exchanged $\delta^{34}S$ values (least negative) give reasonable $\Delta^{18}O_{SO_4-OH}$ temperatures. This indicates that the residence time of aqueous sulfate in solution for some of the samples was sufficient for equilibrium oxygen isotope and significant sulfur isotope exchange between aque-

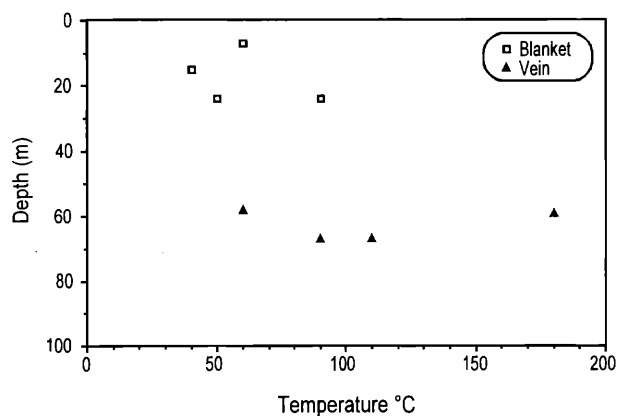


FIG. 9. Depth vs. calculated alunite $\Delta^{18}O_{SO_4-OH}$ temperature for blanket acid leach (open squares) and acid sulfate vein (solid triangles) samples.

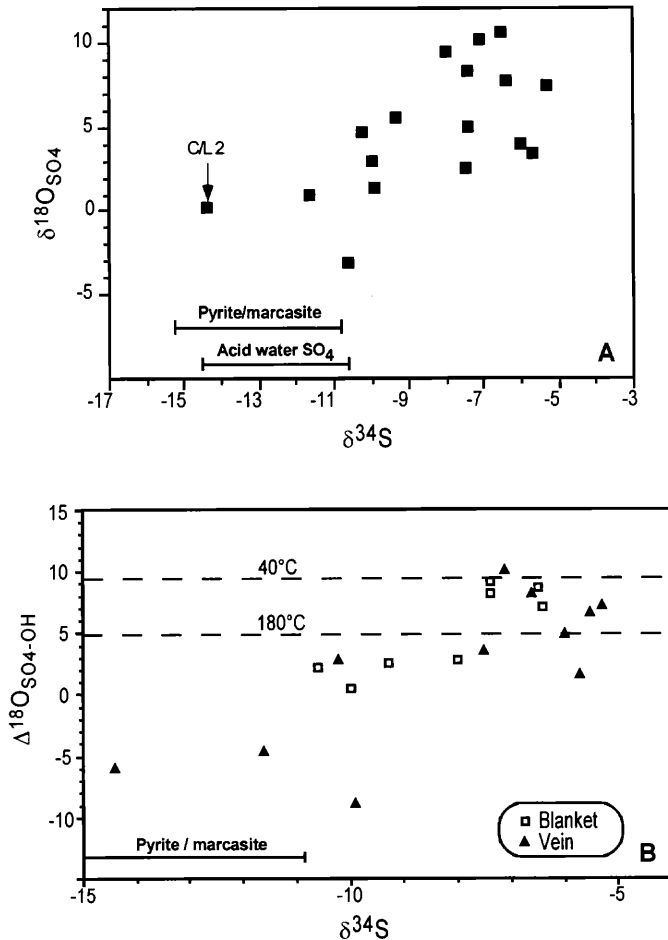


FIG. 10. A. Alunite $\delta^{18}\text{O}_{\text{SO}_4}$ vs. $\delta^{34}\text{S}$. The range of $\delta^{34}\text{S}$ values for early pyrite-marcasite and for acid mine water is also shown. B. The $\Delta^{18}\text{O}_{\text{SO}_4\text{-OH}}$ vs. $\delta^{34}\text{S}$ values of blanket (open squares) and vein alunite (solid triangles) samples. Dashed lines correspond to calculated $\Delta^{18}\text{O}_{\text{SO}_4\text{-OH}}$ temperatures of 40° and 180°C. The $\delta^{34}\text{S}$ range of early pyrite-marcasite is also shown.

ous sulfate and the fluid. The fact that some of the vein alunite samples show a greater degree of S isotope exchange than samples from the blanket zone is consistent with the higher calculated alunite $\Delta^{18}\text{O}_{\text{SO}_4\text{-OH}}$ temperature range in the vein samples. Figure 10B emphasizes that individual samples of steam-heated alunite in which isotopic equilibrium was not attained may not be distinguishable from supergene alunite on the basis of isotopic data alone (Rye et al., 1992).

Jarosite isotopic data

Dark brown, relatively coarsely crystalline jarosite (up to 4 mm) occurs in a veinlet that cuts the blanket acid leach zone (sample C/L 32). Because there is no sulfide or evidence of weathered sulfides above, adjacent to, or immediately below this sample, an origin by supergene oxidation of sulfides is unlikely. This jarosite has an exchanged $\delta^{34}\text{S}$ value of -6.4 per mil and yields a $\Delta^{18}\text{O}_{\text{SO}_4\text{-OH}}$ temperature of 70°C (Rye and Stoffregen, 1995), suggesting a steam-heated origin. In thin section, the jarosite crystals are zoned and are generally transparent with light yellow-green to deep brown pleochro-

ism. Fluid inclusions are rare and typically small (2–5 μm), and identification and measurements are hampered by strong double refraction. Only one reliable homogenization temperature of 87°C was obtained. The sample has an extremely low δD value of -183 per mil due to the large D-H fractionation between jarosite and water (Rye and Stoffregen, 1995). The calculated δD value for the parent fluid is about -120 per mil, consistent with the range in composition of the steam-heated alunite fluids. This sample has a K-Ar age of 0.7 ± 0.2 Ma and represents the youngest known episode of steam-heated alteration.

Two samples of cryptocrystalline jarosite (C/L 33 and C/L 34) consist of light brown fracture coatings that occur in oxidized and unoxidized opal-K feldspar alteration zones which have not been acid leached. Both of these samples have unexchanged $\delta^{34}\text{S}$ values (-11, -13‰) and have very small or negative $\Delta^{18}\text{O}_{\text{SO}_4\text{-OH}}$ values. These jarosites could be supergene. It is quite likely that the oxidation of any shallow sulfides would occur simultaneously with that of H_2S in a shallow geothermal environment.

Source of Sulfur and Hydrocarbons

Sulfides related to primary mineralization and alteration at the Crofoot-Lewis deposit have low $\delta^{34}\text{S}$ values, ranging from -10.8 to -15.2 per mil. These values are very different from those of the local Tertiary volcanic rocks or the underlying metasedimentary Auld Lang Syne Group. One whole-rock $\delta^{34}\text{S}$ analysis from unaltered Tertiary volcanic rocks adjacent to the Crofoot-Lewis mine has a value of 10 per mil. A single sample of pyrite from the Auld Lang Syne Group has a $\delta^{34}\text{S}$ value of -1.9 per mil. Assuming a relatively homogeneous $\delta^{34}\text{S}$, the Auld Lang Syne Group is not a likely source of sulfur for mineralization.

Hydrocarbons or other organic material are typically incorporated into hydrothermal solutions as they pass through sedimentary rocks (Hanor, 1980). Data on $\delta^{34}\text{S}$ values from the late Cenozoic basin sediments adjacent to the Crofoot-Lewis deposit are not available. However, Rice and Tuttle (1989) investigated the $\delta^{34}\text{S}$ values of late Pleistocene to early Holocene age sediments from Walker Lake, in west-central Nevada. Sulfides and organic sulfur in these sediments contain isotopically light sulfur, with $\delta^{34}\text{S}$ values of sulfides ranging from -41.5 to +24.4 per mil, averaging -15.6 per mil (total of 56 samples), and $\delta^{34}\text{S}$ values of organic sulfur ranging from -26.5 to +8.1 per mil and averaging -4.4 per mil (total of 12 samples). Rice and Tuttle's (1989) results show that low $\delta^{34}\text{S}$ values are common in organic matter and sulfide minerals within late Cenozoic basin sediment. H_2S , like hydrocarbons, can be derived from the thermal decomposition of organic matter and hydrocarbons in sedimentary basins (Le Tran et al., 1974). Given sufficient heat, degrading organic matter within the basin sediments could contribute CO_2 , H_2S , and volatile hydrocarbons to the gas phase (Peabody and Einaudi, 1992). Alternatively organic matter and/or hydrocarbons could be incorporated into the recharge fluids and subsequently hydrothermally decomposed (matured) along the flow path.

There are three dominant sedimentary units in the district, the Auld Lang Syne Group, beds within the Black Rock terrane, and the late Cenozoic basin fill. Abundant graphite

within the Auld Lang Syne Group indicates that, at least locally, prior to ore deposition these rocks were subject to temperatures above the oil stability window and are an unlikely source for bitumen. The Black Rock terrane contains igneous and sedimentary rocks, including cherts, mudstones, sandstones, coarse clastic rocks, and minor lacustrine limestones (Oldow, 1984; Russell, 1984). The degree of maturity of hydrocarbons in this unit is unknown. The 2,160-m-thick sequence of late Cenozoic basin sediments that fills the Black Rock Desert basin is considered to be the most likely source of bitumen in the region. As previously mentioned, several of the late Cenozoic basins through Nevada contain showings of oil and gas, and an oil exploration well drilled in the Black Rock Desert basin encountered traces of hydrocarbons above a 2,150-m depth (Garside et al., 1988). Thus, available evidence strongly indicates that the late Cenozoic basin sediments are the source of both bitumen and isotopically light sulfur at the Crofoot-Lewis deposit.

Characteristics of Fluids

Isotopic composition of chloride waters

The term "chloride waters" refers to the deep hydrothermal fluid and is analogous to the neutral pH chloride waters in active geothermal systems (White, 1969; Henley and Ellis, 1983). The isotopic compositions of chloride waters (Fig. 11) have been calculated from $\delta^{18}\text{O}$ values of quartz and calcite using fluid inclusion homogenization temperatures (Ebert, 1995) and $\delta\text{D}_{\text{H}_2\text{O}}$ values determined directly from inclusion fluids. The quartz samples have numerous, but very small (mostly $<2\ \mu\text{m}$) fluid inclusions. The scarcity of sufficiently large fluid inclusions makes determination of accurate filling temperatures problematic and is a possible source of error in the calculated $\delta^{18}\text{O}_{\text{H}_2\text{O}}$ values of the quartz fluids. The stable isotope data on fluids in Figure 11 record a large compositional range in chloride water (calculated from vein

quartz and calcite samples) as well as a large range in surface water (calculated from alunite samples). This range of values could reflect combinations of processes including variations in the isotopic composition of the waters over time, modifications during mixing of deep and shallow waters, boiling, and water-rock interaction. Two of the calculated chloride waters (from quartz) have δD values near -118 per mil. This value falls within the range of early surface water and is the best estimate of an average value for early chloride water. Two calcite and one quartz sample have $\delta\text{D}_{\text{H}_2\text{O}}$ values of fluids ranging from -137 to -153 per mil. The paragenetic relations of these two samples are difficult to demonstrate; however, one of the veins cuts opal-K feldspar alteration and one cuts illite-smectite alteration, therefore both samples are relatively late. The 19 to 35 per mil difference in the $\delta\text{D}_{\text{H}_2\text{O}}$ value between the water for these samples and early chloride water (-118‰) cannot be accounted for by boiling (Truesdell et al., 1977). These low values resulted from mixing of chloride water with a low δD value surface water, or alternatively, the δD value of the chloride waters decreased significantly during the later stages of the system.

A sample of quartz (+ chalcedony) from the mineralized quartz stockwork that cuts the blanket acid leach zone in the Brimstone area has a relatively low $\delta^{18}\text{O}$ value of 4.1 per mil (sample C/L 44). This sample formed very near the present surface, at an estimated temperature between 100° and 120°C (estimated from the hydrostatic boiling point versus depth curve). The calculated range of $\delta^{18}\text{O}_{\text{H}_2\text{O}}$ values for this water are -16.8 to -14.4 per mil, corresponding to low $\delta\text{D}_{\text{H}_2\text{O}}$ values of -158 to -131 per mil from the relationship $\delta\text{D} = 8\delta^{18}\text{O} + 10$ (Craig, 1961).

Oxygen isotope shift in deep thermal waters

The amount of oxygen isotope shift due to water-rock interaction at depth in the deeply circulating geothermal fluid (chloride waters) can be estimated from the $\delta^{18}\text{O}_{\text{H}_2\text{O}} - \delta\text{D}_{\text{H}_2\text{O}}$ value of water that was responsible for vein quartz deposition. The waters that deposited quartz fall along a line parallel to the meteoric water line, but are enriched about 4 per mil in ^{18}O (Fig. 11). This 4 per mil ^{18}O enrichment is attributed to oxygen isotope shift due to water-rock interaction and is similar to that observed in modern geothermal areas such as Yellowstone (Craig et al., 1956; Craig, 1963; Truesdell et al., 1977).

The calcite fluids are enriched about 10 to 11 per mil relative to unexchanged meteoric water. Calcite sample C/L 68 is from a calcite vein that occurs within illite-smectite alteration. Fluid inclusions from this sample have variable liquid to vapor ratios suggestive of boiling (e.g., Bodnar et al., 1985). Some inclusions in this sample have positive melting temperatures (up to 2.6°C) which may result from the formation of clathrate during freezing, indicating the presence of CO_2 or the formation of metastable ice (Roedder, 1984). This sample most likely formed from a CO_2 -rich, steam-heated ground water or a mixture of ground water and chloride water (e.g., Hedenquist, 1990). Calcite sample C/L 69 is from a dark brown to black, coarsely banded calcite \pm chalcedony vein. Fluid inclusions from this sample are also dominantly two phase with variable liquid to vapor ratios. The increase in ^{18}O shift in these calcite fluids over that for the quartz

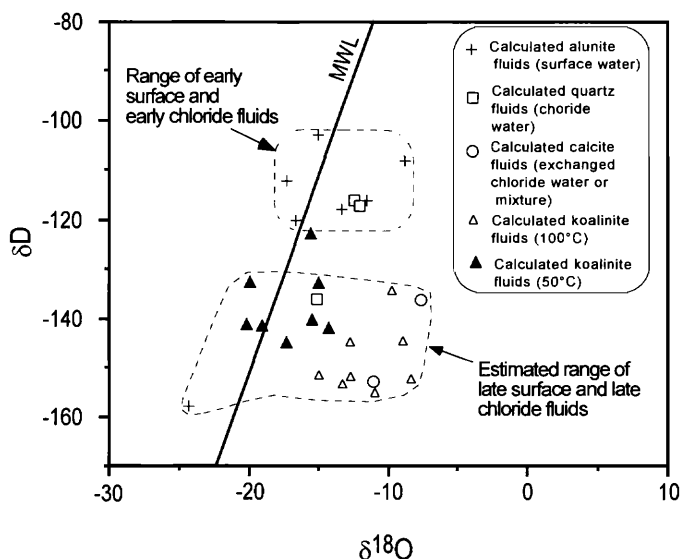


FIG. 11. Fluid $\delta\text{D}_{\text{H}_2\text{O}}$ and $\delta^{18}\text{O}_{\text{H}_2\text{O}}$ values for deep and shallow fluids calculated from alunite δD and $\delta^{18}\text{O}$ values and $\Delta^{18}\text{O}_{\text{SO}_4-\text{OH}}$ temperatures, and quartz and calcite $\delta^{18}\text{O}$ values, fluid inclusion $\delta\text{D}_{\text{H}_2\text{O}}$ values, and homogenization temperatures.

fluids is possibly due to isotopic enrichment during boiling (Truesdell et al., 1977) or during interaction of CO₂-rich steam-heated waters with the country rock, as described at the Broadlands-Ohaaki geothermal systems, New Zealand (Simmons and Christenson, 1994).

Isotopic composition of acid sulfate waters

Isotopic compositions of waters that deposited alunite can be calculated from temperature information and the fractionation factors of Stoffregen et al. (1994). Figure 11 shows the calculated isotopic compositions of water in equilibrium with those alunites that yield reasonable $\Delta^{18}\text{O}_{\text{SO}_4\text{-OH}}$ temperatures. The δD and $\delta^{18}\text{O}$ values of alunite water plot near the meteoric water line, and most have δD values between -100 and -123 per mil, which is close to the value of chloride water and is consistent with the average value (-120‰) interpreted to have been typical of meteoric water in this area back to the late Tertiary (Friedman et al., 1993). Alunite waters which plot to the right of the meteoric water line could be due to evaporation in the steam-heated environment (Ellis and Mahon, 1977; Truesdell et al., 1977).

The fluid for one alunite has a δD value of -158 per mil and along with the corresponding $\delta^{18}\text{O}_{\text{H}_2\text{O}}$ value plots near the meteoric water line (Fig. 11). This alunite was collected from a remnant mud pool near the top of the blanket acid leach zone and, based on its position in the system, it is younger than the other alunite samples (although its K-Ar age indicates that it is slightly older). The low $\delta\text{D}_{\text{H}_2\text{O}}$ value for this alunite sample cannot be accounted for by temperature-related fractionation or evaporation, and it was almost certainly deposited from an isotopically light surface water. This isotopically light surface water is consistent with the composition of the late chloride waters presented above.

Postdepositional D exchange in kaolinites and δD of late-stage fluids

With one exception (alunite C/L 1), all kaolinite δD values are 41 to 50 per mil lower than those of associated alunites (Fig. 8). Based on the fractionation factors of alunite-H₂O (Stoffregen et al., 1994) and kaolinite-H₂O (Liu and Epstein, 1984), there is little difference between δD values of alunite and kaolinite which formed from the same fluid at temperatures above 150°C. Since $\Delta^{18}\text{O}_{\text{SO}_4\text{-OH}}$ temperatures calculated for alunite indicate that several of the samples formed at temperatures between 40° and 180°C, and the alunite and kaolinite appear to have been deposited contemporaneously, the greater than 40 per mil difference in δD values between coexisting alunite and kaolinite cannot be explained by temperature-related fractionation. We suggest that δD values of the fine-grained kaolinites have been reset by exchange with late, isotopically light fluids. Experimental studies show that kaolinite is susceptible to low-temperature H exchange in the absence of significant O isotope exchange (O'Neil and Kharaka, 1976; Kyser and Kerrich, 1991). The mechanism involves exchange with OH site and is distinct from the D-H changes that accompany recrystallization or neof ormation, both of which are associated with changes in $\delta^{18}\text{O}$ values.

The kaolinite samples analyzed in this study are very fine grained, typically less than 1 μm , and are therefore suscepti-

ble to H isotope exchange with a late, isotopically light hydrothermal fluid (O'Neil and Kharaka, 1976). Figure 12 shows that the δD values of kaolinites from the veins are slightly depleted in D relative to kaolinites from the blanket zone. One interpretation of this trend is that kaolinites in the veins reached a greater degree of isotopic equilibrium with an overprinting fluid than kaolinites in the blanket zone. This difference would be consistent with higher elevation of the blanket zone which most likely resulted in lower temperatures or a shorter duration of contact with an overprinting hydrothermal fluid.

The observation that H isotope exchange in kaolinite requires the influx of fluids having a substantially lower $\delta\text{D}_{\text{H}_2\text{O}}$ value than that of the primary fluids, and along with the low δD value of alunite C/L 1, suggests low $\delta\text{D}_{\text{H}_2\text{O}}$ values for fluids late in the life of the geothermal system.

Relation of Mineralization to Paleoclimate

The Crofoot-Lewis deposit records large fluctuations in both the isotopic composition of fluids and in the level of the paleowater table over time. These changes can be correlated with Pliocene to Pleistocene paleoclimate records for the western United States and are therefore interpreted to reflect major climate changes over the life of the system.

Studies of marine oxygen isotope, foraminiferal, and diatom records, combined with terrestrial taxa and other indicators (Thompson, 1991), suggest that from approximately 4.8 to 2.4 Ma relatively high rainfall and mild temperatures existed in the western United States. This wetter climate created several large lakes throughout western North America (Forester, 1991). At about 2.4 Ma, the first large continental glaciation events occurred in the northern hemisphere, and these cooler temperatures and greater aridity lasted from 2.4 to about 2.0 Ma (Thompson, 1991). From 2.0 to about 1.8 Ma, warmer and moister conditions prevailed through western North America (Thompson, 1991).

Detailed studies of late Cenozoic perennial lake deposits from Searles Lake, California, by Smith (1984) demonstrated six distinct paleohydrologic conditions in the Great Basin over the past 3.2 m.y.: 3.2 to 2.5 Ma (wet); 2.5 to 2.0 Ma (dry);

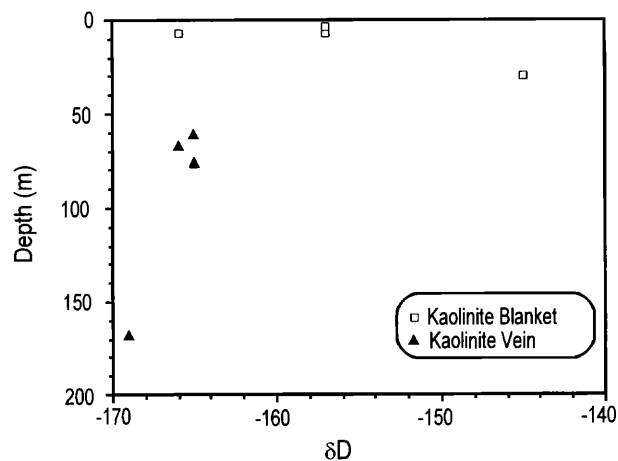


FIG. 12. Depth vs. δD for kaolinite from the blanket acid leach zone and acid sulfate veins.

2.0 to 1.3 Ma (intermediate); 1.3 to 1.0 Ma (wet), 1.0 to 0.6 Ma (intermediate); 0.6 to 0.3 Ma (dry).

The various episodes of alteration at the Crofoot-Lewis deposit between 4 to 0.7 Ma and the δD values of meteoric water correlate well with this paleoclimate record. A possible history of the system based on the combined paleoclimate studies of Thompson (1991) and Smith (1984) is presented below and is illustrated schematically in Figure 13:

1. 4.8 to 2.5 or 2.4 Ma: wet conditions and mild temperatures created a lake in the Black Rock Desert basin. Geothermal activity began during this interval, and fluid discharge near the margin of the lake, focused along range-bounding normal faults, resulted in widespread near-surface opal-K feldspar alteration and sinter deposition (Fig. 13A).

2. 2.5 or 2.4 to 2.0 Ma: lower temperatures and more arid conditions associated with glaciation at high elevations resulted in a reduced size of the lake in the Black Rock Desert basin (Fig. 13B). The resulting drop (18 m minimum) in the water table enabled steam-heated acid sulfate alter-

ation to overprint opal-K feldspar alteration, resulting in secondary Au-Ag-enriched zones that are economically mineable. During the later part of this period, δD values of fluids decreased from about -120 to -158 per mil.

3. 2.0 to 1.3 Ma: warmer, moister intermediate conditions resulted in a rise in the lake level and water table allowing the geothermal system to overprint the near-surface blanket acid leach alteration (Fig. 13C). The high water table, possibly related to glacial melt water, enabled a late episode of mineralized quartz stockwork veining to reach the near-surface, locally overprinting and mineralizing blanket acid leach alteration in the Brimstone area and resetting kaolinite to lower δD values.

4. 1.3 to 1.0 Ma: relatively wet conditions may have resulted in a further rise in the water-table (at least 50 m above the lowest water table level during the second episode).

5. 1.0 to 0.6 Ma: intermediate and dry conditions again resulted in an increase in δD values of meteoric waters (-120‰) and a possible drop in the lake level and the water table (Fig. 13D). Late (0.7 Ma) steam-heated jarosite formed

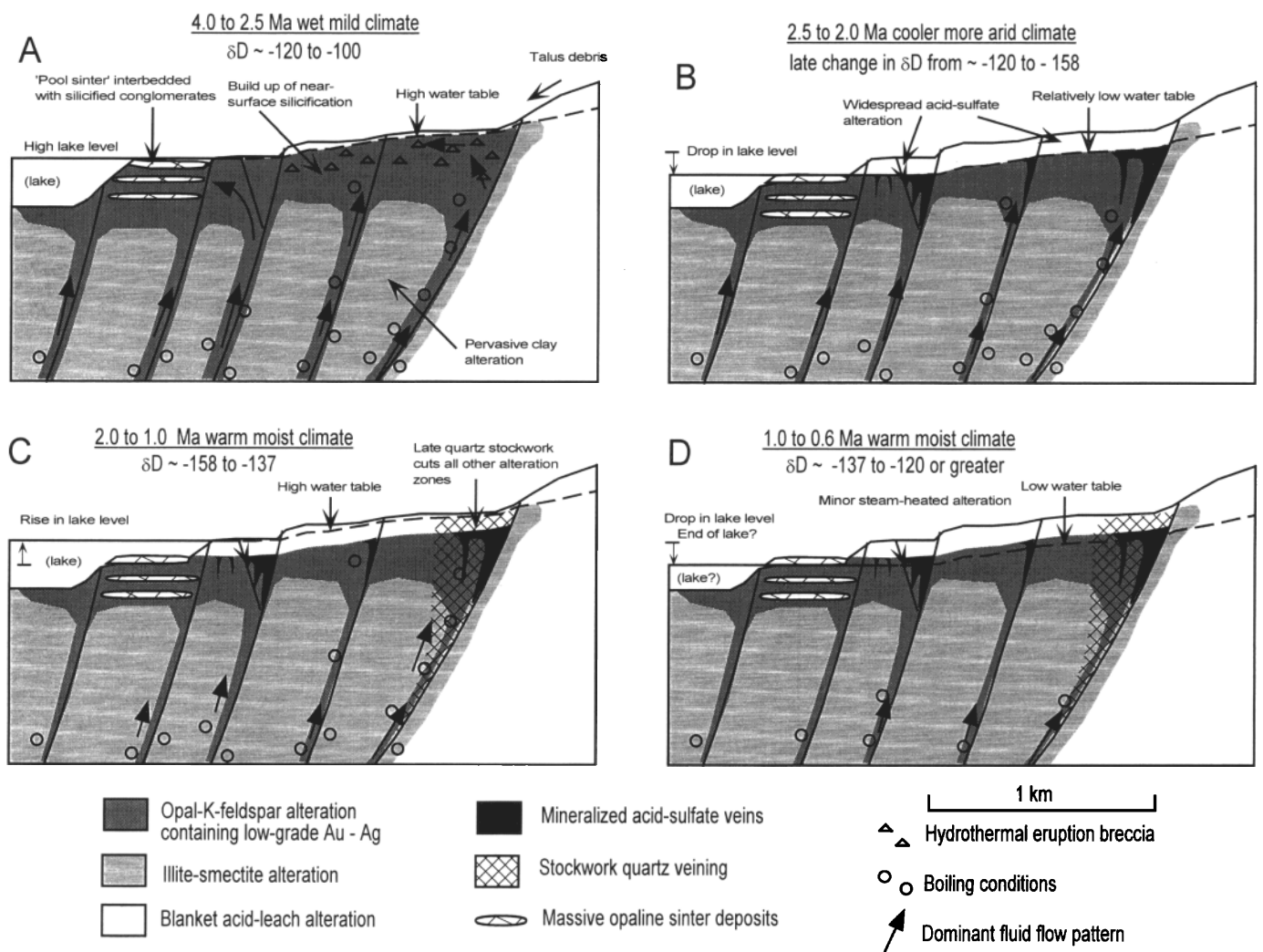


FIG. 13. Schematic cross section through the Crofoot-Lewis deposit showing formation through time and interpreted changes in δD values (see text).

along fractures above the water table in the blanket acid leach zone.

6. 0.6 to 0.3 Ma: dry conditions caused a further drop in the water table. Geothermal activity probably ceased during this time. Current warm waters and H₂S gas in the area probably reflect conductive heating.

Factors other than climatic conditions could account for the observed fluctuations in the paleowater table. However, as the known variations in paleoclimate can explain both the fluctuations in the water table and the variable δD values, changes in paleoclimate are considered to be the best explanation of the δD -time data at the Crofoot-Lewis deposit.

Fluid Circulation Model

This section proposes a simple convection model for the Crofoot-Lewis system in which meteoric water flowed along extensional fractures in the basin and was heated mainly by the high thermal gradient in the region. This model is consistent with the S isotope data and the apparent longevity of the Crofoot-Lewis system, but is admittedly speculative, mainly because of a lack of geophysical data on the basin, the paucity and uncertainty of the radiometric age data on the Crofoot-Lewis deposit, and the lack of supporting hydrologic modeling studies. Nevertheless, it is important to present this model, because, if correct, the potential area that can be targeted for exploration of young hot spring gold deposits in the Great Basin increases significantly. Figure 14 is a specula-

tive cross section through the Sulphur region that is consistent with all of the data available from the area.

Most active geothermal systems and epithermal ore deposits are associated in time and space with subaerial volcanism, and an igneous heat source is often demonstrated or inferred (Henley, 1985). Figure 14, however, is drawn without an igneous heat source, although the model does not require the absence of such a heat source. The Crofoot-Lewis deposit and several geothermal systems in northern Nevada are somewhat anomalous in that they lack obvious coeval volcanism (Crewdson, 1976; Blackwell, 1983). Many authors consider the high geothermal gradient in northern Nevada to be sufficient to account for most of the present geothermal systems in the region (Hose and Taylor, 1974; Sass et al., 1979; Blackwell, 1983; Buchanan, 1990).

The region surrounding the Sulphur district falls within the Battle Mountain high, an area of anomalous heat flow in the northern Basin and Range province that has a geothermal gradient of about 50°C/km (Duffield et al., 1994). The voluminous deposits of silica sinter at the Crofoot-Lewis mine indicate deposition by fluids from a reservoir with a temperature greater than 210°C (Fournier, 1985). Since the depth to the brittle-ductile transformation near central Pershing County is between 12 and 18 km (Catchings, 1992), meteoric waters should be able to circulate easily to deeper than 4 km and be heated only by the high geothermal gradient to reach temperatures above 210°C as shown in Figure 14.

Seismic reflection and refraction data from northwest Ne-

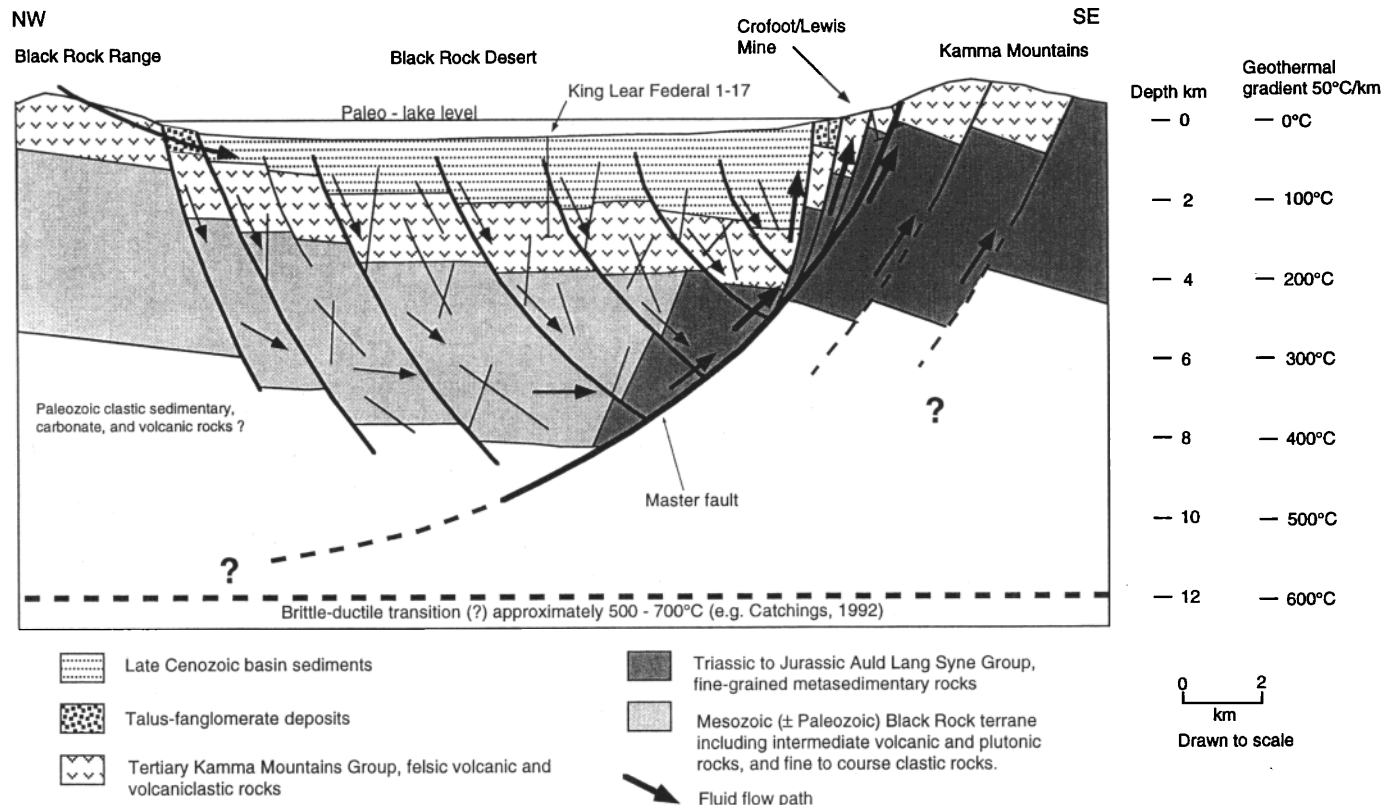


FIG. 14. Simplified interpretive cross section through the Black Rock Desert and adjacent ranges, showing interpreted geology and hydrothermal fluid convection. An igneous heat source is not shown but could be present.

vada indicate that the major range-bounding faults flatten with depth and that the intensity of faulting and fracturing is much greater within basins than in adjacent ranges (Catchings, 1992). Seismic reflection, gravity, and geologic data from the Dixie valley area, Nevada, also show the ranges to be composed of a fairly solid block, whereas the adjacent basins are highly faulted and fractured to depths of 15 to 20 km (Okaya, 1985). The simplified structure presented in Figure 14 illustrates the high density of faulting and fracturing inferred to occur below the Black Rock Desert basin.

The high density of faulting within the basins provides pathways for the downward migration of meteoric water (e.g., Hose and Taylor, 1974). Fluid convection is favored in fractured rocks with high permeability that are exposed to a geothermal gradient (Criss and Hofmeister, 1991). Convective flow can be caused by the inverse density gradient that results from the thermal expansion of water, such that hot fluid is displaced upward by the inward flow of cooler, denser fluid (Criss et al., 1991; Bjørlykke, 1993). In Figure 14 recharge for the system is shown to occur within the basin with upflow along the range-bounding faults at the basin margins as proposed by Mase and Sass (1980) from their study of the Black Rock Desert area.

Fluid discharge, and the localization of geothermal activity and epithermal mineralization in northern Nevada, is commonly restricted to the range-bounding faults along the pediment at the basin margins. Geophysical studies show that many basins in northern Nevada are highly asymmetrical, with the deeper side adjacent to the dominant or master fault and the other side marked by valleyward tilt and a complex series of antithetic faults (Stewart, 1971). We predict that the more significant and deeper penetrating master faults have a significant role in focusing deep fluid upflow (and perhaps heat-flow from depth), and therefore exert a major control on the distribution of epithermal and geothermal systems in the basin-and-range setting.

Summary

Radiogenic isotope ages suggest that the Crofoot-Lewis system was long-lived, with at least intermittent activity for over 3 m.y. Field evidence indicates that the blanket acid leach zone at the Crofoot-Lewis deposit formed in a steam-heated environment in a geothermal system. Stable isotope data confirm a steam-heated origin for this zone.

Sulfate for the acid sulfate alteration was generated by oxidation of H₂S in the vadose zone, but $\delta^{34}\text{S}$ values of sulfates reflect the degree of sulfur isotope exchange with H₂S in the system. Calculated alunite $\Delta^{18}\text{O}_{\text{SO}_4-\text{OH}}$ temperatures also vary through the acid sulfate alteration zone depending on the degree to which aqueous sulfate reached oxygen isotope equilibrium with water in the system. The δD values of fluids are typical of meteoric water and a rather large range of such values reflects changing climate conditions during the life of the hydrothermal system.

A fluctuating water table enabled acid sulfate waters to overprinted low-grade opal-K feldspar mineralization resulting in the leaching, redistribution, and concentration of Au and Ag. These Au-Ag zones are associated with opal + alunite + kaolinite + montmorillonite \pm hematite and formed in open-space fractures below the paleowater table.

The paleoclimate was an important factor in the formation of the Crofoot-Lewis deposit by controlling the level of the paleowater table and the availability of meteoric recharge water. During periods of high surface water availability, the highly fractured areas beneath the basins are interpreted to be favorable sites for meteoric water convection. Meteoric waters recharged along faults through the late Cenozoic basin sediments, acquiring S and hydrocarbons. These deeply circulating geothermal fluids were eventually focused and discharged along basin-and-range faults near the margin of a lake. An igneous heat source is possible but not apparent at the system, and it is suggested that the high regional geothermal gradient was sufficient to form the ore deposit, with fluids circulating to minimum depths of 4 km.

Acknowledgments

Discussions with David Groves helped develop the concepts proposed in this paper, and his editing and review is greatly appreciated. David John and Ted McKee from the United States Geological Survey performed K-Ar analyses on alunite samples and one illite sample from the Crofoot-Lewis deposit and made these samples available for stable isotope analyses; their sharing of data and ideas is greatly appreciated. Discussions with Brad Wigglesworth, Ken Jones, Alain Cotnoir, and Frederick Felder have significantly contributed to the ideas presented in this paper. We acknowledge reviews by Byron Berger, Phil Bethke, Jeff Doebrich, Al Hofstra, David John, Ed Mikucki, Stuart Simmons, and *Economic Geology* referees that have contributed significantly to improving this manuscript. Several of the gas extractions, isotopic analyses, and countless other tasks were done in the laboratory by Carol Gent, and her contributions at the U.S.G.S. stable isotope laboratory in Denver are greatly appreciated. Hycroft Resources and Development Inc. and Granges Inc. provided financial support for the project. Additional support was provided by the Key Centre for Strategic Mineral Deposits and an Overseas Postgraduate Research Scholarship at the University of Western Australia.

November 6, 1995; June 26, 1997

REFERENCES

- Barton, P.B., Bethke, P.M., and Roedder, E., 1977, Environment of ore deposition in the Creede mining district, San Juan Mountains, Colorado: Part III. Progress toward interpretation of the chemistry of the ore-forming fluid for the OH vein: *ECONOMIC GEOLOGY*, v. 72, p. 1-24.
- Berger, B.R., and Henley, R.W., 1989, Advances in the understanding of epithermal gold-silver deposits, with special reference to the western United States: *ECONOMIC GEOLOGY MONOGRAPH* 6, p. 405-423.
- Bjørlykke, K., 1993, Fluid flow in sedimentary basins: *Sedimentary Geology*, v. 86, p. 137-158.
- Blackwell, D.B., 1983, Heat flow in the northern Basin and Range province: Geothermal Resources Council Special Report 13, p. 81-91.
- Bodnar, R.J., Reynolds, T.J., and Kuehn, C.A., 1985, Fluid-inclusion systematics in epithermal systems: *Reviews in Economic Geology*, v. 2, p. 73-97.
- Browne, P.R.L., 1978, Hydrothermal alteration in active geothermal fields: *Annual Review of Earth and Planetary Science*, v. 6, p. 229-250.
- Buchanan, P.K., 1990, Determination of timing of recharge for geothermal fluids in the Great Basin using environmental isotopes and paleoclimate indicators: Unpublished M.Sc. thesis, University of Nevada-Reno, 115 p.
- Burke, D.B., and Silberling, N.J., 1974, The Auld Lang Syne Group of Late Triassic and Jurassic age, north-central Nevada: *U.S. Geological Survey Bulletin* 1394-E.
- Catchings, R.D., 1992, A relation among geology, tectonics, and velocity

- structure, western to central Nevada Basin and Range: *Geological Society of America Bulletin*, v. 104, p. 1178–1192.
- Craig, H., 1961, Isotopic variations in meteoric waters: *Science*, v. 133, p. 1702–1703.
- 1963, The isotopic chemistry of water and carbon, in geothermal areas, in Tongiorgi, E., ed., *Nuclear geology on geothermal areas—Spoleto: Pisa, Italy, Consiglio Nazionale Delle Ricerche, Laboratorio di Geologia Nucleare*, p. 17–53.
- Craig, H., Boato, G., and White, D.W., 1956, Isotopic geochemistry of thermal waters: National Academy of Science, Natural Resources Council Publication 400, p. 29–38.
- Crewdson, R.A., 1976, Geophysical studies in the Black Rock Desert geothermal prospect, Nevada: Unpublished Ph.D. thesis, Colorado School of Mines, 180 p.
- Criss, R.E., and Hofmeister, A.M., 1991, Application of fluid dynamics principles in tilted permeable media to terrestrial hydrothermal systems: *Geophysical Research Letters*, v. 18, no. 2, p. 199–202.
- Criss, R.E., and Taylor, H.P., Jr., 1986, Meteoric-hydrothermal systems: *Reviews in Mineralogy*, v. 16, p. 373–424.
- Criss, R.E., Fleck, R.J., and Taylor, H.P., 1991, Tertiary meteoric hydrothermal systems and their relation to ore deposition, northwestern United States and southern British Columbia: *Journal of Geophysical Research*, v. 96, no. B8, p. 13335–13356.
- Cronin, T.M., Cannon, W.F., and Poore, R.Z., 1983, Paleoclimate and mineral deposits: U.S. Geological Survey Circular 882, 59 p.
- Duffield, W.A., Sass, J.H., and Sorey, M.L., 1994, Tapping the earth's natural heat: U.S. Geological Survey Circular 1125, 63 p.
- Ebert, S.W., 1995, The anatomy and origin of the Crofoot-Lewis mine, a low-sulfidation hot-spring type gold-silver deposit located in northwest Nevada: Unpublished Ph.D. thesis, Nedlands, Western Australia, University of Western Australia.
- Ebert, S.W., Groves, D.I., and Jones, J.K., 1996, Geology, alteration, and ore controls of the Crofoot-Lewis mine, Sulphur, Nevada: A well-preserved hot-spring gold-silver deposit: *Geological Society of Nevada Symposium, Reno-Sparks, Nevada, April 1995, Proceedings*, p. 209–234.
- Ellis, A.J., and Mahon, W.A.J., 1977, *Chemistry and geothermal systems*: New York, Academic Press, 392 p.
- Forester, R.M., 1991, Pliocene-climate history of the western United States derived from lacustrine ostracodes: *Quaternary Science Reviews*, v. 10, p. 133–146.
- Foley, N.K., Bethke, P.M., and Rye, R.O., 1989, A reinterpretation of the δD_{H_2O} of inclusion fluids in contemporaneous quartz and sphalerite, Creede mining district, Colorado: A generic problem of shallow orebodies?: *ECONOMIC GEOLOGY*, v. 84, p. 1966–1977.
- Fournier, R.O., 1985, The behavior of silica in hydrothermal solutions: *Reviews in Economic Geology*, v. 2, p. 45–62.
- Friedman, I., Gleason, J., and Warden, A., 1993, Ancient climate from deuterium content in volcanic glass: Climate change in continental isotopic records: *Geophysical Union Monograph* 78, p. 309–319.
- Garside, L.J., Hess, R.H., Fleming, K.L., and Weimer, B.S., 1988, Oil and gas developments in Nevada: Nevada Bureau of Mines and Geology Bulletin 104, 136 p.
- Guilbert, J.M., and Park, C.F., Jr., 1986, *The geology of ore deposits*: New York, W.H. Freeman and Company, 985 p.
- Hanor, J.S., 1980, Dissolved methane in sedimentary brines: Potential PVT properties of fluid inclusions: *ECONOMIC GEOLOGY*, v. 75, p. 603–609.
- Heald, P., Foley, N.K., and Hayba, D.O., 1987, Comparative anatomy of volcanic-hosted epithermal deposits: Acid-sulfate and adularia-sericite types: *ECONOMIC GEOLOGY*, v. 82, p. 1–26.
- Hedenquist, J.W., 1987, Mineralization associated with volcanic-related hydrothermal systems in the circum-Pacific basin: Circum-Pacific Energy and Mineral Resources Conference, 4th, Singapore, Transactions, p. 513–524.
- 1990, The thermal and geochemical structure of the Broadlands-Ohaaki geothermal system, New Zealand: *Geothermics*, v. 19, no. 2, p. 151–185.
- Hedenquist, J.W., and Browne, P.R.L., 1989, The evolution of the Waitapu geothermal system, New Zealand, based on the chemical and isotopic composition of its fluids, minerals and rocks: *Geochimica et Cosmochimica Acta*, v. 53, p. 2235–2257.
- Hedenquist, J.W., Matsuhisa, Y., Izawa, E., White, N.C., Giggenback, W.F., and Aoki, M., 1994, Geology, geochemistry, and origin of high-sulfidation Cu-Au mineralization in the Nansatsu district, Japan: *ECONOMIC GEOLOGY*, v. 89, p. 1–30.
- Hemley, J.J., and Jones, W.R., 1964, Chemical aspects of hydrothermal alteration with emphasis on hydrogen metasomatism: *ECONOMIC GEOLOGY*, v. 59, p. 538–569.
- Henley, R.W., 1985, The geothermal framework of epithermal deposits: *Reviews in Economic Geology*, v. 2, p. 1–24.
- Henley, R.W., and Ellis, A.J., 1983, Geothermal systems, ancient and modern: *Earth-Science Reviews*, v. 19, p. 1–50.
- Henley, R.W., and McNabb, A., 1978, Magmatic vapor plumes and ground-water interaction in porphyry copper emplacement: *ECONOMIC GEOLOGY*, v. 73, p. 1–20.
- Henneberger, R.C., and Browne, P.R.L., 1988, Hydrothermal alteration and evolution of the Ohakuri hydrothermal system, Taupo volcanic zone, New Zealand: *Journal of Volcanology and Geothermal Research*, v. 34, p. 211–231.
- Holland, H.D., 1965, Some applications of thermochemical data to problems of ore deposits. II. Mineral assemblages and the composition of ore-forming fluids: *ECONOMIC GEOLOGY*, v. 60, p. 1101–1166.
- Hose, R.K., and Taylor, B.E., 1974, Geothermal systems of northern Nevada: U.S. Geological Survey Open-File Report 74–271, 27 p.
- Johnson, M.G., 1977, Geology and mineral deposits of Pershing County, Nevada: Nevada Bureau of Mines and Geology Bulletin 89, 115 p.
- Kyser, T.K., and Kerrich, R., 1991, Retrograde exchange of hydrogen isotopes between hydrous minerals and water at low temperatures: *Geochemical Society Special Publication* 3, p. 409–422.
- Lawrence, J.R., and Taylor, H.P., 1971, Deuterium and oxygen-18 correlation: Clay minerals and hydroxides in Quaternary soils compared to meteoric waters: *Geochimica et Cosmochimica Acta*, v. 35, p. 993–1003.
- Le Tran, K., Connan, J., and Vanderweide, B., 1974, Diagenesis of organic matter and occurrences of hydrocarbons and H₂S in the SW Aquitaine basin (France): *Centre de Recherche, Pau-SNPA, Bulletin*, v. 8, p. 111–137.
- Listova, L.P., Vainshtein, A.Z., and Ryabinina, A.A., 1968, Dissolution of gold in media forming during oxidation of some sulphides [abs.]: *Chemical Abstracts*, v. 68, 88967h.
- Liu, K.K., and Epstein, S., 1984, The hydrogen isotope fractionation between kaolinite and water: *Isotope Geoscience*, v. 2, p. 335–350.
- Mann, A.W., 1984, Mobility of gold and silver in lateritic weathering profiles: Some observations from Western Australia: *ECONOMIC GEOLOGY*, v. 79, p. 38–49.
- Marumo, K., Matsuhisa, Y., and Nagasawa, K., 1982, Hydrogen and oxygen isotopic compositions of kaolin minerals in Japan: *Developments in Sedimentology*, no. 35, p. 315–320.
- Mase, C.W., and Sass, J.H., 1980, Heat flow from the western arm of the Black Rock Desert, Nevada: U.S. Geological Survey Open-File Report 80–1238, 38 p.
- Morrison, R.B., 1964, Lake Lahontan: Geology of southern Carson Desert, Nevada: U.S. Geological Survey Professional Paper 401, 156 p.
- Ohmoto, H., and Rye, R.O., 1979, Isotopes of sulfur and carbon, in Barnes, H.L., ed., *Geochemistry of hydrothermal ore deposits*: New York, Wiley Interscience, p. 509–567.
- Okaya, D.A., 1985, Seismic reflection studies in the Basin and Range province and Panama: Unpublished Ph.D. thesis, Stanford, California, Stanford University, 133 p.
- Oldow, J.S., 1984, Evolution of a late Mesozoic back-arc fold and thrust belt, northwestern Great Basin, U.S.A.: *Tectonophysics*, v. 102, p. 245–274.
- O'Neil, J.R., and Kharaka, Y.K., 1976, Hydrogen and oxygen isotope exchange reactions between clay minerals and water: *Geochimica et Cosmochimica Acta*, v. 40, p. 241–246.
- Parnell, J., 1993, Introductory comments: *Society for Geology Applied to Mineral Deposits Special Publication* 9, p. 1–7.
- Parry, W.T., Ballantyne, J., Bryant, N., and Dedolph, R., 1980, Geochemistry of hydrothermal alteration at the Roosevelt Hot Springs thermal area, Utah: *Geochimica et Cosmochimica Acta*, v. 44, p. 95–102.
- Peabody, C.E., and Einaudi, 1992, Origin of petroleum and mercury in the Culver-Baer cinnabar deposit, Mayacmas district, California: *ECONOMIC GEOLOGY*, v. 87, p. 1078–1103.
- Rice, C.A., and Tuttle, M.L., 1989, Sulfur speciation and isotopic analyses of sediment samples from Walker Lake, Nevada: U.S. Geological Survey Open-File Report 89–4, 14 p.
- Roedder, E., 1984, Fluid inclusions: *Reviews in Mineralogy*, v. 12, 644 p.
- Russell, B.J., 1984, Mesozoic geology of the Jackson Mountains, northwestern Nevada: *Geological Society of America Bulletin*, v. 95, p. 313–323.

- Rye, R.O., 1993, The evolution of magmatic fluids in the epithermal environment: The stable isotope perspective: *ECONOMIC GEOLOGY*, v. 88, p. 733–753.
- Rye, R.O., Bethke, P.M., and Wasserman, M.D., 1992, The stable isotope geochemistry of acid sulfate alteration: *ECONOMIC GEOLOGY*, v. 87, p. 225–262.
- Rye, R.O., and Stoffregen, R.E., 1995, Experimental determination of jarosite-water oxygen and hydrogen isotope fractionations: *ECONOMIC GEOLOGY*, v. 90, p. 2336–2342.
- Rye, R.O., Bethke, P.M., and Wasserman, M.D., 1992, The stable isotope geochemistry of acid sulfate alteration: *ECONOMIC GEOLOGY*, v. 87, p. 225–262.
- Sass, J.H., Zoback, M.L., and Galanis, S.P., Jr., 1979, Heat flow in relation to hydrothermal activity in the southern Black Rock Desert, Nevada: U.S. Geological Survey Open-File Report 79–1467, 43 p.
- Savin, S.M., and Epstein, S., 1970, The oxygen and hydrogen isotope geochemistry of clay minerals: *Geochimica et Cosmochimica Acta*, v. 34, p. 24–42.
- Schoen, R., White, D.E., and Hemley, J.J., 1974, Argillization by descending acid at Steamboat Springs, Nevada: *Clays and Clay Minerals*, v. 22, p. 1–22.
- Simmons, S.F., 1991, Hydrologic implications of alteration and fluid inclusion studies in the Fresnillo district, Mexico: Evidence for a brine reservoir and a descending water table during formation of hydrothermal Ag-Pb-Zn orebodies: *ECONOMIC GEOLOGY*, v. 86, p. 1579–1601.
- Simmons, S.F., and Christenson, 1994, Origins of calcite in a boiling geothermal system: *American Journal of Science*, v. 294, p. 361–400.
- Smith, G.I., 1984, Paleohydrologic regimes in the southwestern Great Basin, 0–3.2 my ago, compared with other long records of “Global” climate: *Quaternary Research*, v. 22, p. 1–17.
- Stewart, J.H., 1971, Basin and Range structure: A system of horsts and grabens produced by deep-seated extension: *Geological Society of America Bulletin*, v. 82, p. 1019–1044.
- 1980, *Geology of Nevada*: Nevada Bureau of Mines and Geology Special Publication 4, 136 p.
- Stoffregen, R., 1986, Observations on the behavior of gold during supergene oxidation at Summitville, Colorado, U.S.A., and implications for electrum stability in the weathering environment: *Applied Geochemistry*, v. 1, p. 549–558.
- 1987, Genesis of acid sulfate alteration and Au-Cu-Ag mineralization at Summitville, Colorado: *ECONOMIC GEOLOGY*, v. 82, p. 1575–1591.
- Stoffregen, R.E., Rye, R.O., and Wasserman, D.M., 1994, Experimental studies of alunite I. ^{18}O - ^{16}O and D-H fractionation factors between alunite and water at 250–450°C: *Geochimica et Cosmochimica Acta*, v. 58, p. 903–916.
- Taylor, H.P., Jr., 1979, Oxygen and hydrogen isotope relationships in hydrothermal mineral deposits, in Barnes, H.L., ed., *Geochemistry of hydrothermal ore deposits*: New York, Wiley Interscience, p. 236–277.
- Thompson, R.S., 1991, Pliocene environments and climates in the western United States: *Quaternary Science Reviews*, v. 10, p. 115–132.
- Truesdell, A.H., Nathenson, M., and Rye, R.O., 1977, The effects of subsurface boiling and dilution on the isotopic compositions of Yellowstone thermal waters: *Journal of Geophysical Research*, v. 82, p. 3694–3704.
- Vikre, P.G., 1985, Precious metal vein systems in the National district, Humboldt County, Nevada: *ECONOMIC GEOLOGY*, v. 80, p. 360–393.
- Wallace, A.B., 1987, *Geology of the Sulphur district, southwest Humboldt County, Nevada*: Geological Society of Nevada Symposium, Reno, Nevada, 1987, Guidebook for Field Trips, p. 165–171.
- Webster, J.G., 1986, The solubility of gold and silver in the system Au-Ag-S-O₂-H₂O at 25°C and 1 atm.: *Geochimica et Cosmochimica Acta*, v. 50, p. 1837–1845.
- 1987, Thiosulphate in surficial geothermal waters, North Island, New Zealand: *Applied Geochemistry*, v. 2, p. 579–584.
- Webster, J.G., and Mann, A.W., 1984, The influence of climate, geomorphology and primary geology on the supergene migration of gold and silver: *Journal of Geochemical Exploration*, v. 22, p. 21–42.
- White, D.E., 1969, Thermal and mineral waters of the United States—a brief review of possible origins: *International Geological Congress, 23rd, Czechoslovakia, 1969*, v. 19, p. 269–286.
- White, D.E., Hutchinson, R.A., and Keith, T.E., 1988, The geology and remarkable thermal activity of Norris Geyser basin, Yellowstone National Park, Wyoming: U.S. Geological Survey Professional Paper 1456, 84 p.
- Willden, R., 1964, *Geology and mineral deposits of Humboldt County, Nevada*: Nevada Bureau of Mines and Geology Bulletin 59, 154 p.